FORMATION AND CHARACTERISATION OF NANOSTRUCTURED METASTABLE ALLOYS

Viorel Pop
Faculty of Physics, Babes-Bolyai University, 3400 Cluj-Napoca, Romania

Nanocrystalline materials obtained by:

- vapour - inert gas condensation, sputtering, plasma processing, vapour deposition
- liquid - electrodeposition, ***rapid solidification***
- solid - ***mechanical alloying***, severe plastic deformation, spark erosion

mechanical alloying
and
rapid quenching

nanostructured **hard** **and** **soft** **magnetic materials**

ANNEALING modifies
the structure and microstructure

mechanical alloying
and
rapid quenching

Metastable phases

Ï Thermodynamic equilibrium conditions

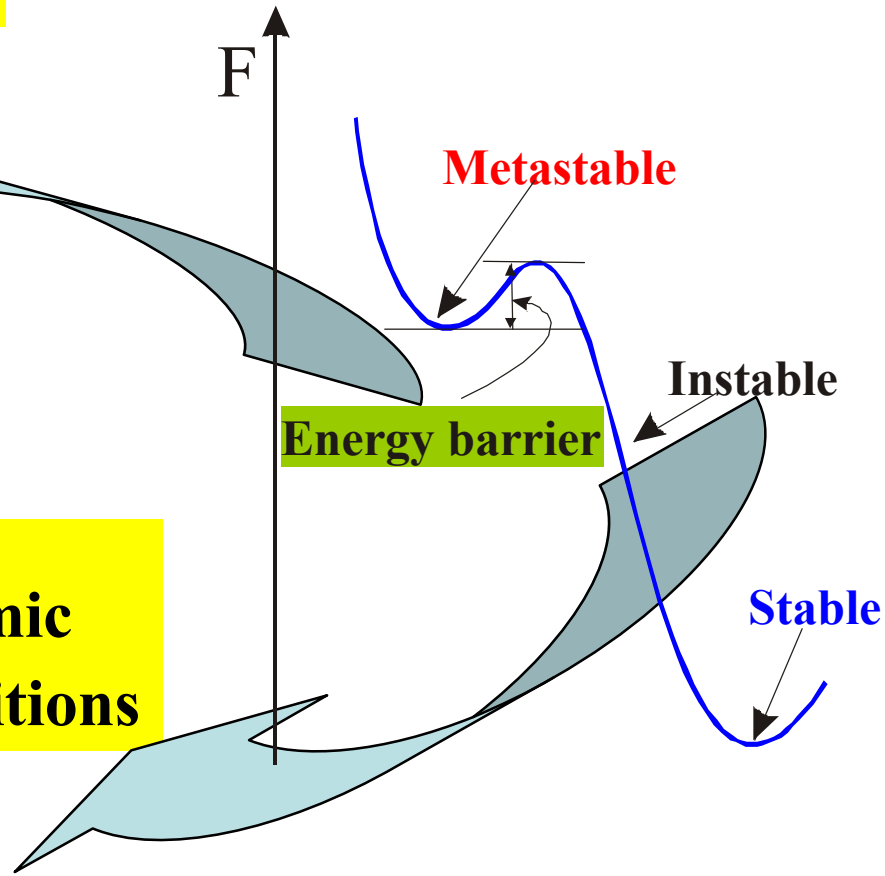

Nanocrystalline structures can be obtained

- **directly**
- **amorphous precursors**

Generally, there are three empirical requirements which must be satisfied by magnetic alloys to produce amorphous precursor

1. **The alloys are composed of more than three elements.**
2. **The constituent alloying elements have significantly different atom size.**
3. **The heat formation of the amorphous alloys is negative.**

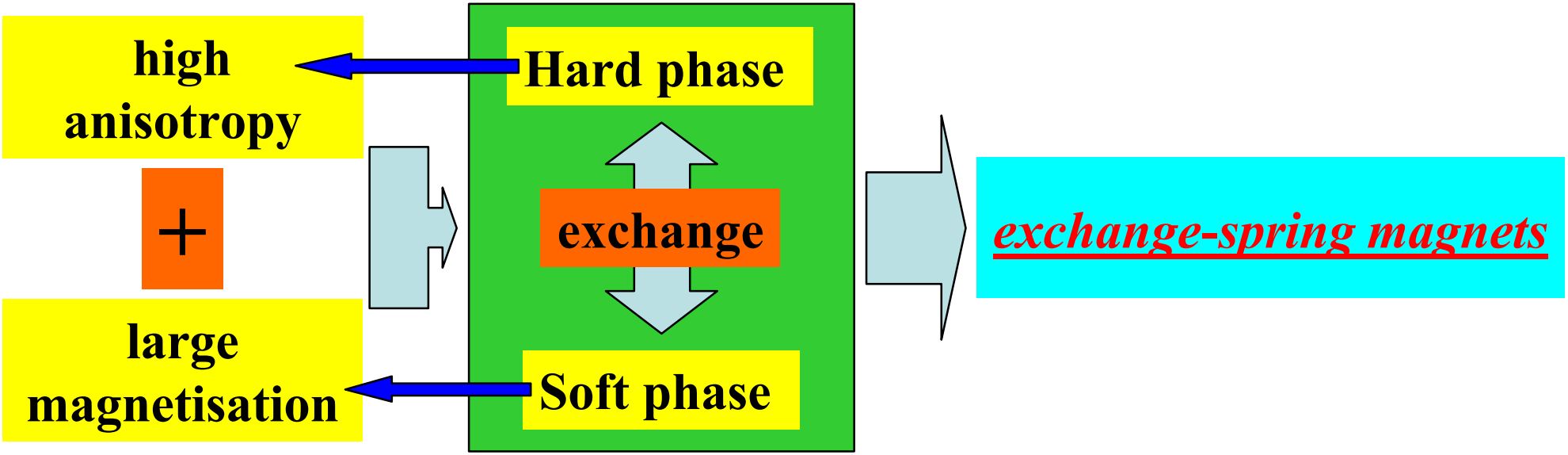
high anisotropy
+
large magnetisation
Hard phase
exchange
Soft phase
exchange-spring magnets

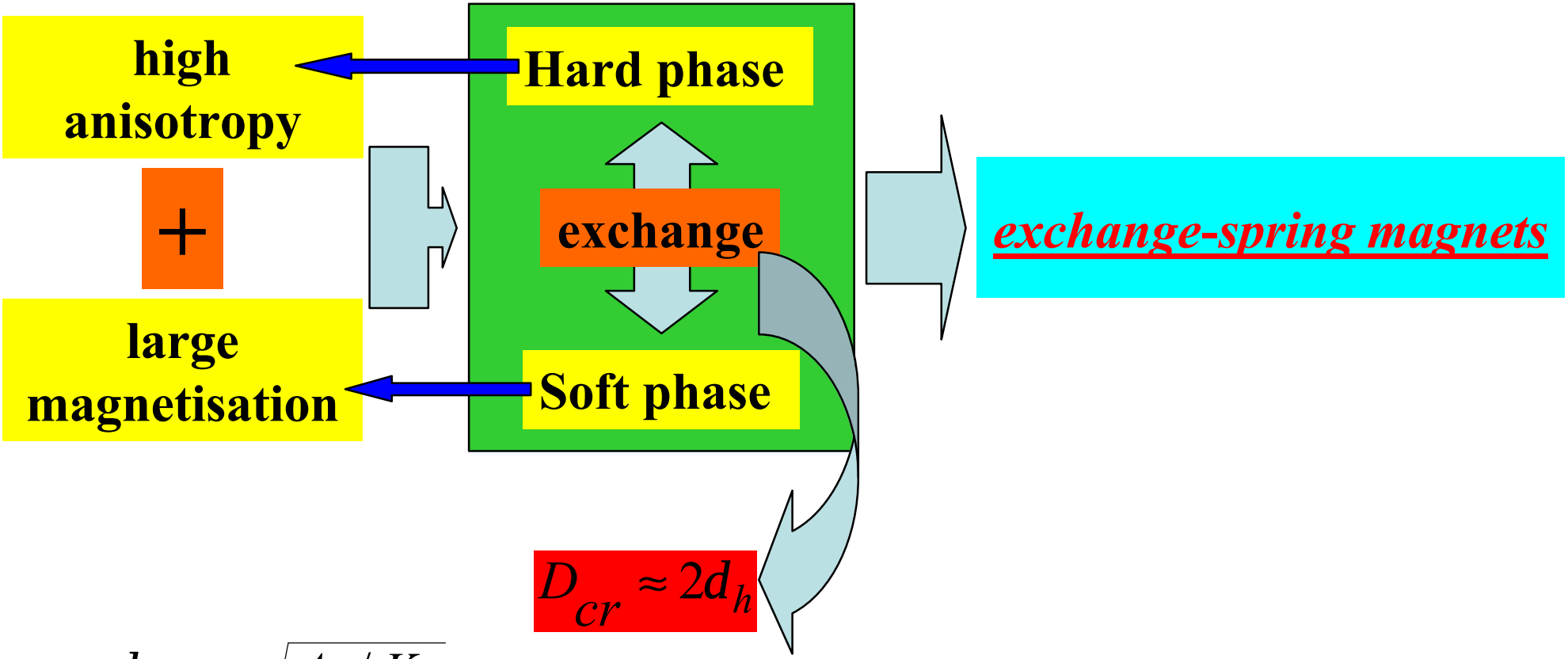

$$d_h = p\sqrt{A_h / K_h}$$

$\boldsymbol{D}_{\mathbf{cr}}$ = soft phase critical dimension

$d_{\mathbf{h}}$ = width of domain wall in the hard phase

$\boldsymbol{A}_{\mathbf{h}}$ and $\boldsymbol{K}_{\mathbf{h}}$ are the exchange and anisotropy constants

Large reversible demagnetization curve

+

A strength remanence $m_r > 0.5$ ($m_r = M_r/M_s$)

EXPERIMENTAL
criteria for the presence of the
exchange spring mechanism

In hard magnetic nanocrystalline materials full or almost full crystallization is required.

Nanocrystalline
soft magnetic materials

→ **partial crystallisation**

↓

two-phase materials

a nanocrystalline + **an amorphous matrix**

Nanocrystalline
soft magnetic materials

→ **partial crystallisation**

→ **two-phase materials**

a nanocrystalline + **an amorphous matrix**

↓ **negative magnetostriction**

compensates

↓ **positive magnetostriction**

Nanocrystalline
soft magnetic materials

→ **partial crystallisation**

→ **two-phase materials**

a nanocrystalline + **an amorphous matrix**

↓ **negative magnetostriction**

compensates

↓ **positive magnetostriction**

for Fe ⇨ V_{cr} »**70-75 %**

Nanocrystalline soft magnetic materials → **partial crystallisation**

→ **two-phase materials**

a nanocrystalline + **an amorphous matrix**

a nanocrystalline → **negative magnetostriction**

an amorphous matrix → **positive magnetostriction**

compensates

for Fe ⇨ V_{cr} »**70-75 %**

$$D < L_{ex}; \qquad L_{ex} = \sqrt{A / 4pM_s^2}$$

D = nanocrystallite diameter

L_{ex} = magnetic exchange length

Nanocrystalline soft magnetic materials → **partial crystallisation**

two-phase materials

a nanocrystalline + **an amorphous matrix**

negative magnetostriction — **compensates** — **positive magnetostriction**

for Fe ⇨ V_{cr} »**70-75 %**

$$D < L_{ex}; \qquad L_{ex} = \sqrt{A / 4pM_s^2}$$

D = nanocrystallite diameter

L_{ex} = magnetic exchange length

G. **Herzer**, IEEE Trans. Magn. MAG-25 (1989) 3327; IEEE Trans. Magn. MAG-26 (1990) 1397

***D*<15 nm**
for a-Fe(Si) and a-Fe nanocrystals present in
Finemet ($Fe_{73.5}Cu_1Nb_3Si_{13.5}B_9$)
and respectively
Nanoperm ($Fe_{84}Zr_{3.5}Nb_{3.5}B8Cu_1$)

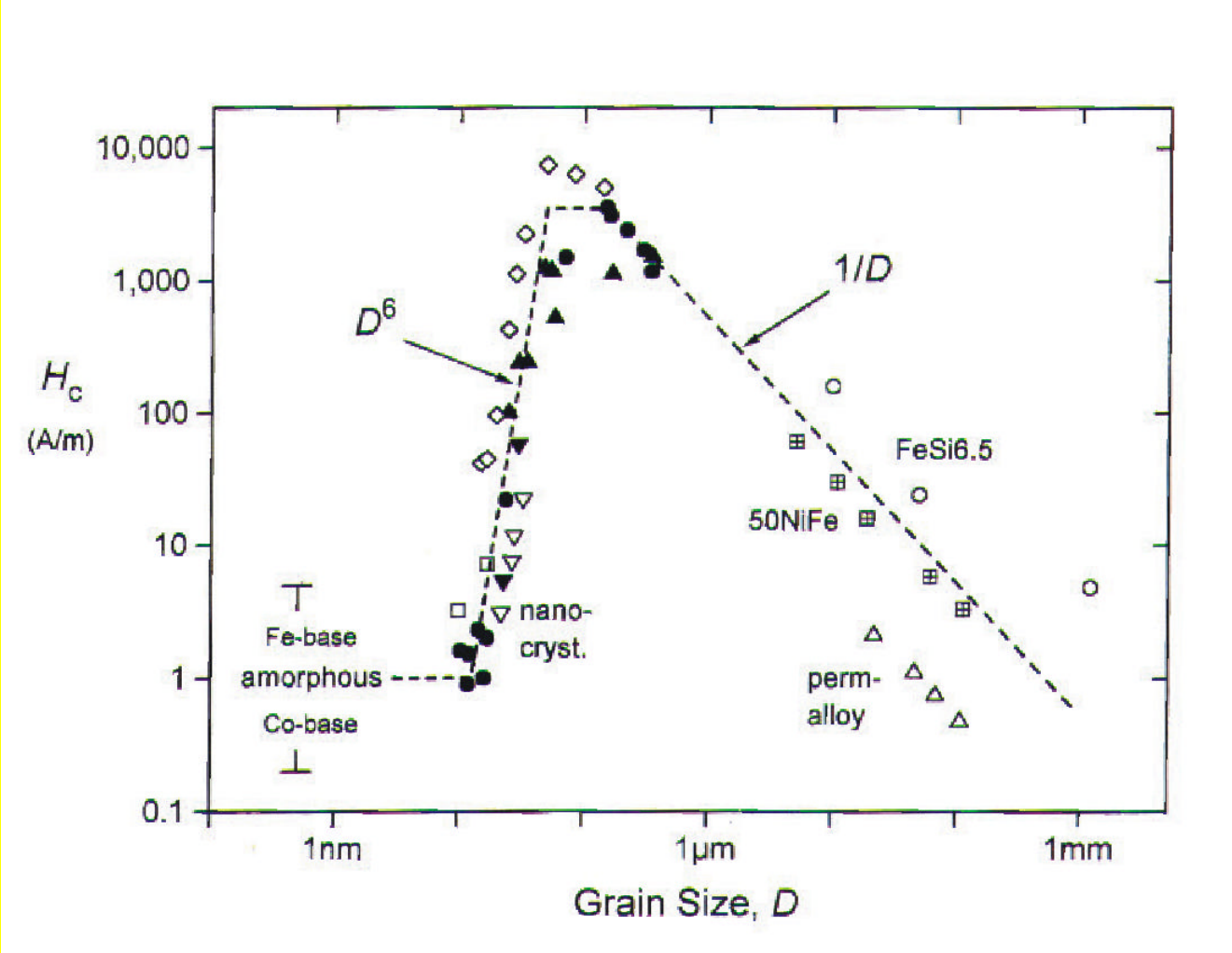
10,000
1,000
100
10
1
0.1
H_c
(A/m)
D^6
1/D
FeSi6.5
50NiFe
nano-
cryst.
Fe-base
amorphous
Co-base
perm-
alloy
1nm
1μm
1mm
Grain Size, D

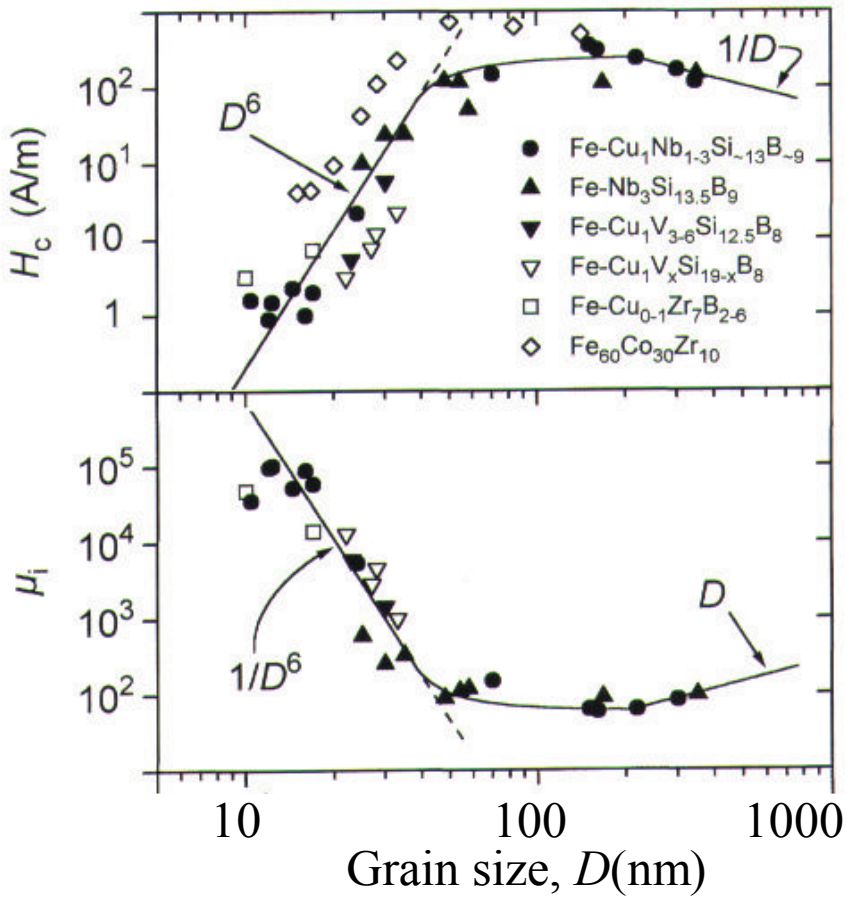
H_c (A/m)
10^2
10^1
10
1
D^6
1/D
Fe-Cu$_1$Nb$_{1-3}$Si$_{\sim 13}$B$_{\sim 9}$
Fe-Nb$_3$Si$_{13.5}$B$_9$
Fe-Cu$_1$V$_{3-6}$Si$_{12.5}$B$_8$
Fe-Cu$_1$V$_x$Si$_{19-x}$B$_8$
Fe-Cu$_{0-1}$Zr$_7$B$_{2-6}$
Fe$_{60}$Co$_{30}$Zr$_{10}$
μ_i
10^5
10^4
10^3
10^2
$1/D^6$
D
10
100
1000
Grain size, D(nm)

vanish of the coercivity in superparamagnetic regime → **low permeability**

soft magnetic nanostructures

↓

small ferromagnetic crystallites coupled by exchange interactions → **low coercivity and high permeability**

The local anisotropies are randomly averaged out by exchange interactions so that there is no anisotropy net effect on the magnetisation process.

Rapid quenching

Nanocrystalline structure is obtained 2 steps:

1. **Formation of the amorphous state by rapid quenching of liquid alloy at very high cooling rate of 10^5-10^6 K/s.**
2. **Partial or complete crystallisation of the amorphous alloy by annealing.**

Rapid quenching

Nanocrystalline structure is obtained 2 steps:

1. **Formation of the amorphous state by rapid quenching of liquid alloy at very high cooling rate of 10^5-10^6 K/s.**
2. **Partial or complete crystallisation of the amorphous alloy by annealing.**

Spin melting

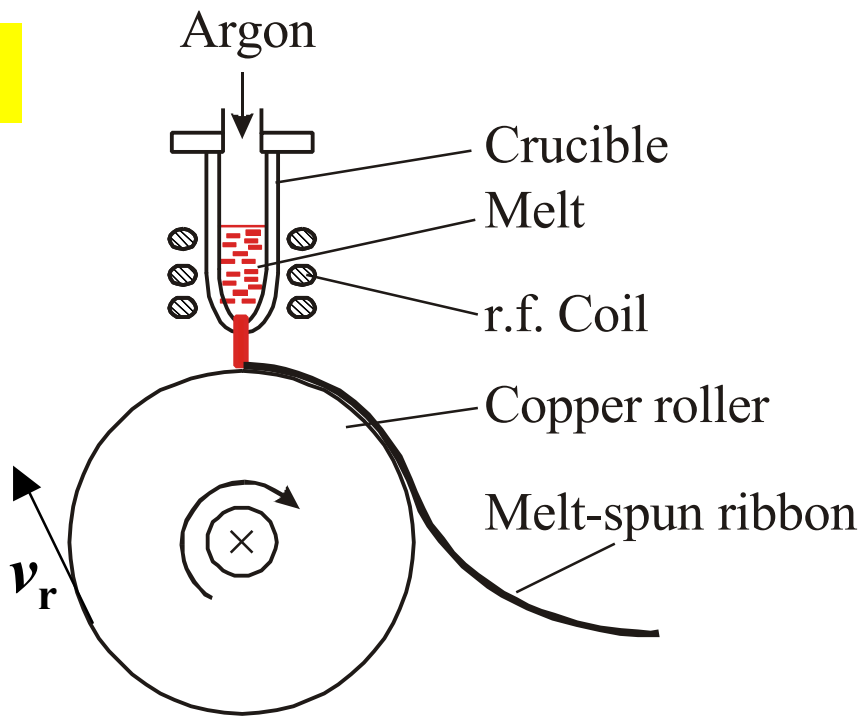

v_r = 20 -30 m/s

v_r = 80 m/s !!!

Table 1. General characteristics of the soft and hard magnetic materials produced by annealing of metallic glasses.

Nanocrystalline materials	Magnetically soft (Fe-based)	Magnetically hard (Fe-based)
Alloys	Finemet $(Fe_{73.5}Cu_1Nb_3Si_{13.5}B_9)$ Nanoperm $(Fe_{84}Zr_{3.5}Nb_{3.5}B_8Cu_1)$ Hitperm $(Fe_{44}Co_{44}Zr_7B_4Cu_1)$	R-Fe-B R = rare-earth e.g. $Nd_{11.8}Fe_{82.3}B_{5.9}$ $Pr_5Fe_{88}Nb_2B_5$
Structure	Nanocrystals (bcc-Fe)+ amorphous matrix	Nanocrystals $Nd_2F_{14}B$+ (Fe_3B, a-Fe, amorphous)
V_{cr}	70–75 % $\Rightarrow \lambda_s \approx 0^*$	$\leq$ 100 %
D	$\leq$ 15 nm $\Rightarrow$ $\langle K \rangle$: 0**	< 25 nm
Properties	High permeability, low magnetic losses	High coercivity, high remanence

*λ_s–saturation magnetostriction constant

** $\langle K \rangle$averaged magnetocrystalline anisotropy

T. **Kulik**, J. Non Crystalin Solids 287 (2001) 145

Spin melting
SOFT

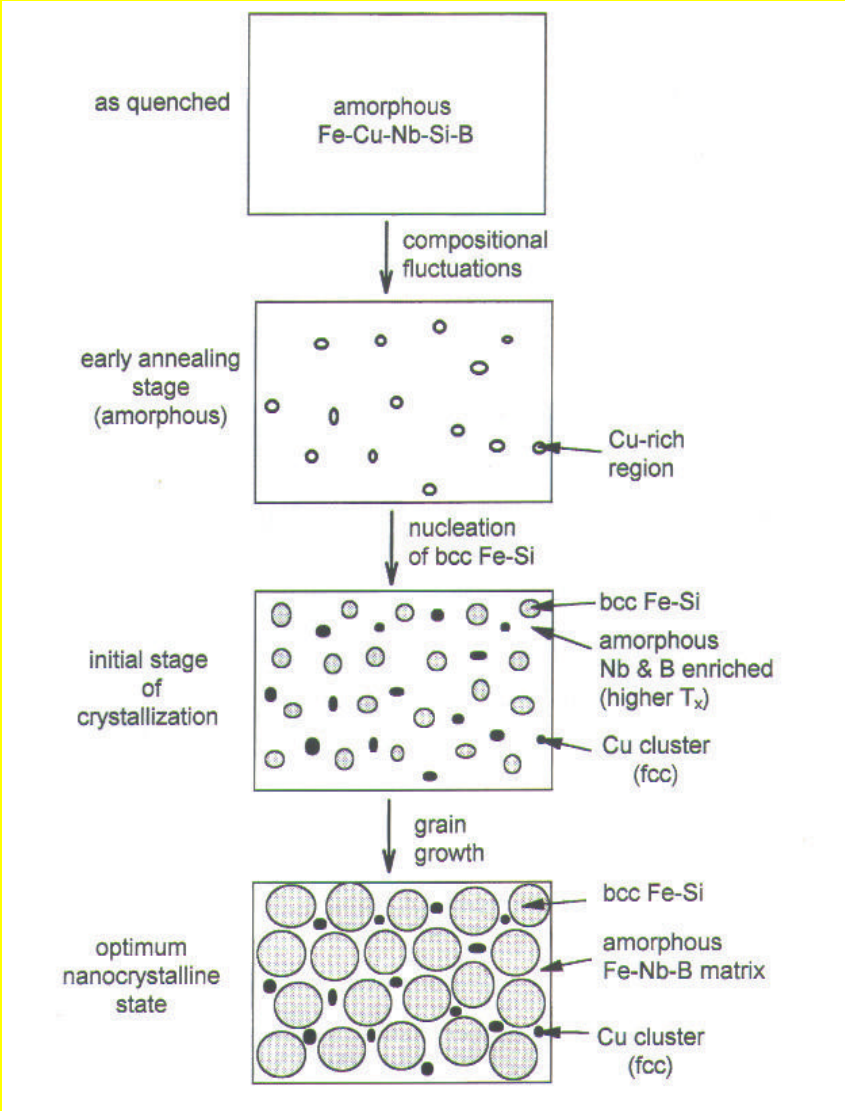

Inhibits the formation of Fe boride compounds

↑

Nb

↓

Promote the formation of Cu-rich clusters

↓

Increase the density of Fe nucleation in between Cu-clusters

Schematic illustration of the formation of the nanocrystalline structure in Fe-Cu-Nb-Si-B alloys based on atom probe analysis results and TEM

G. Herzer, Handbook of Mag. Mater., Ed. K.H.J. Buschow, Vol 10 (1997) 415

Spin melting SOFT

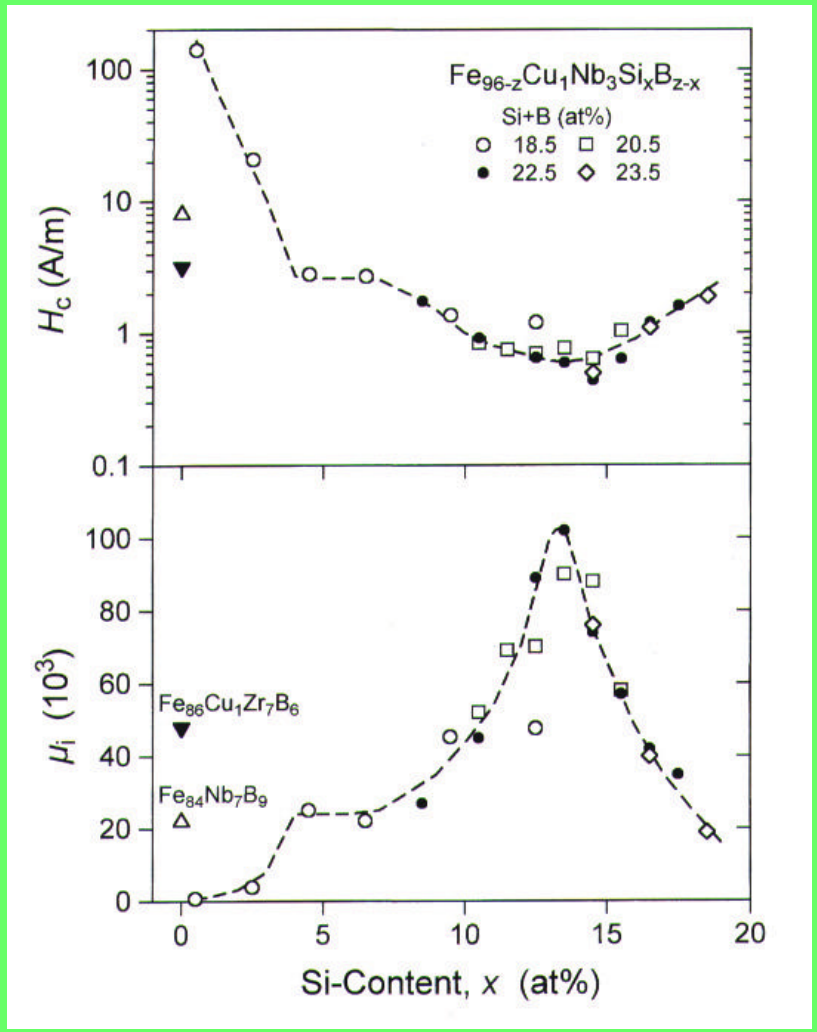

Annealed 1h/540 °C

G. **Herzer**, Handbook of Mag. Mater., Ed. K.H.J. Buschow, Vol 10 (1997) 415

Spin melting SOFT

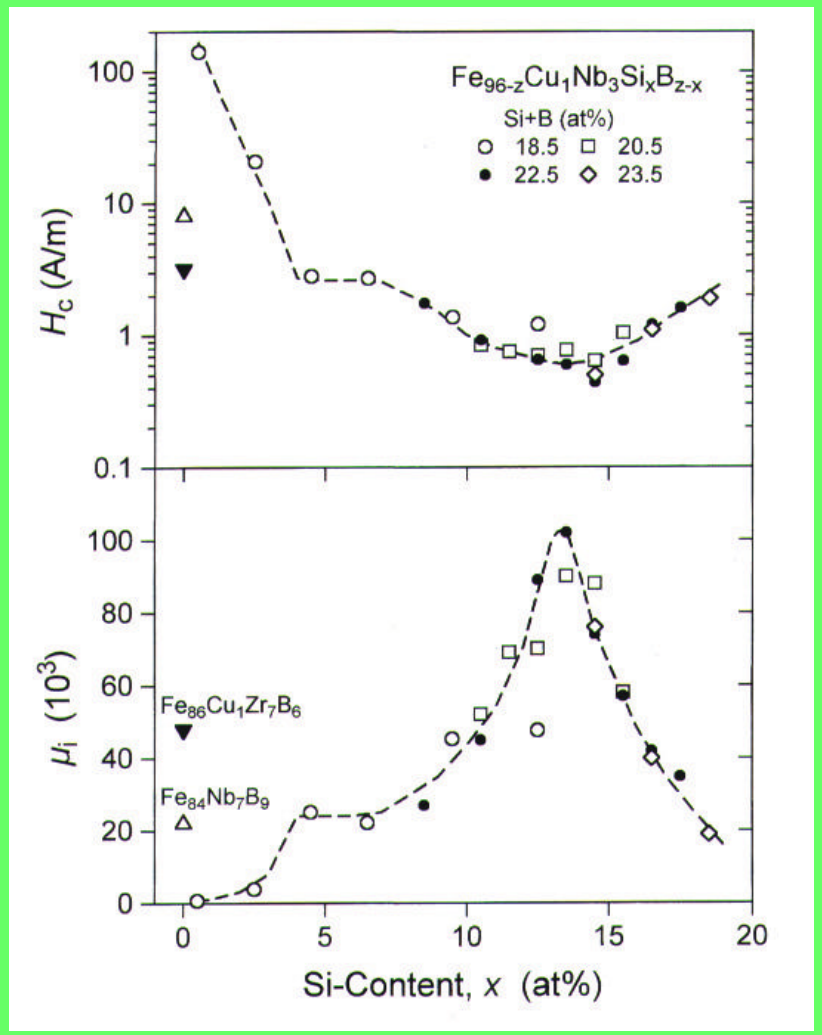

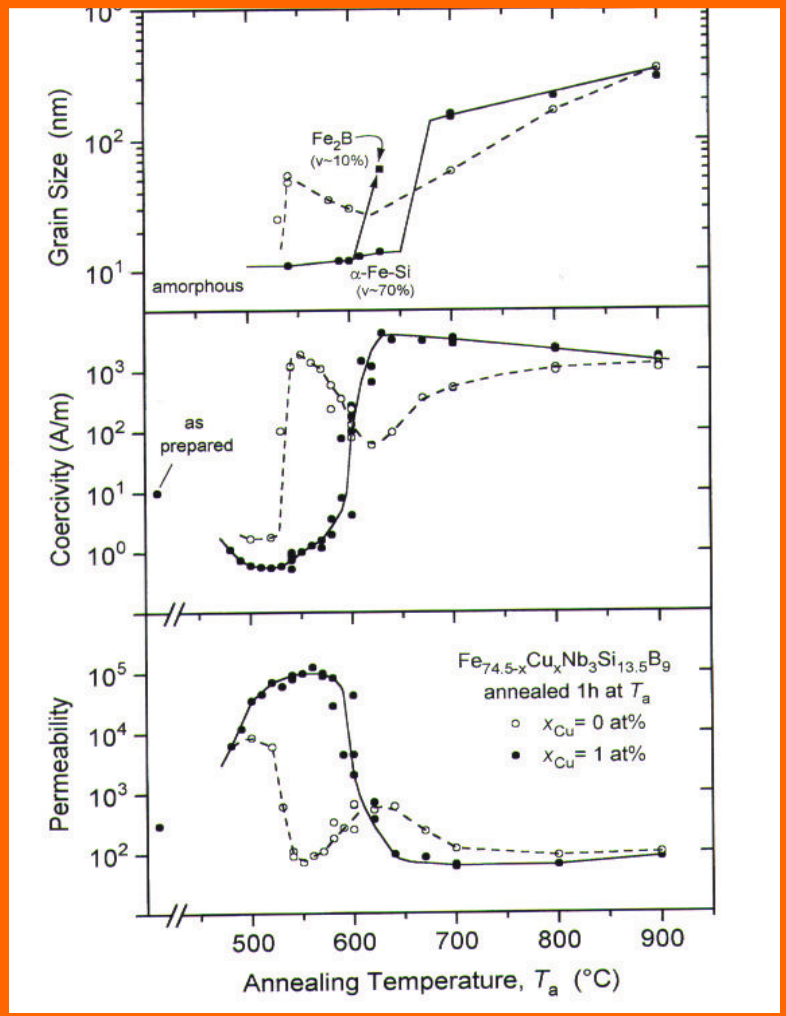

Annealed 1h/540 °C

G. **Herzer**, Handbook of Mag. Mater., Ed. K.H.J. Buschow, Vol 10 (1997) 415

Spin melting SOFT

DTA – differential thermal analysis

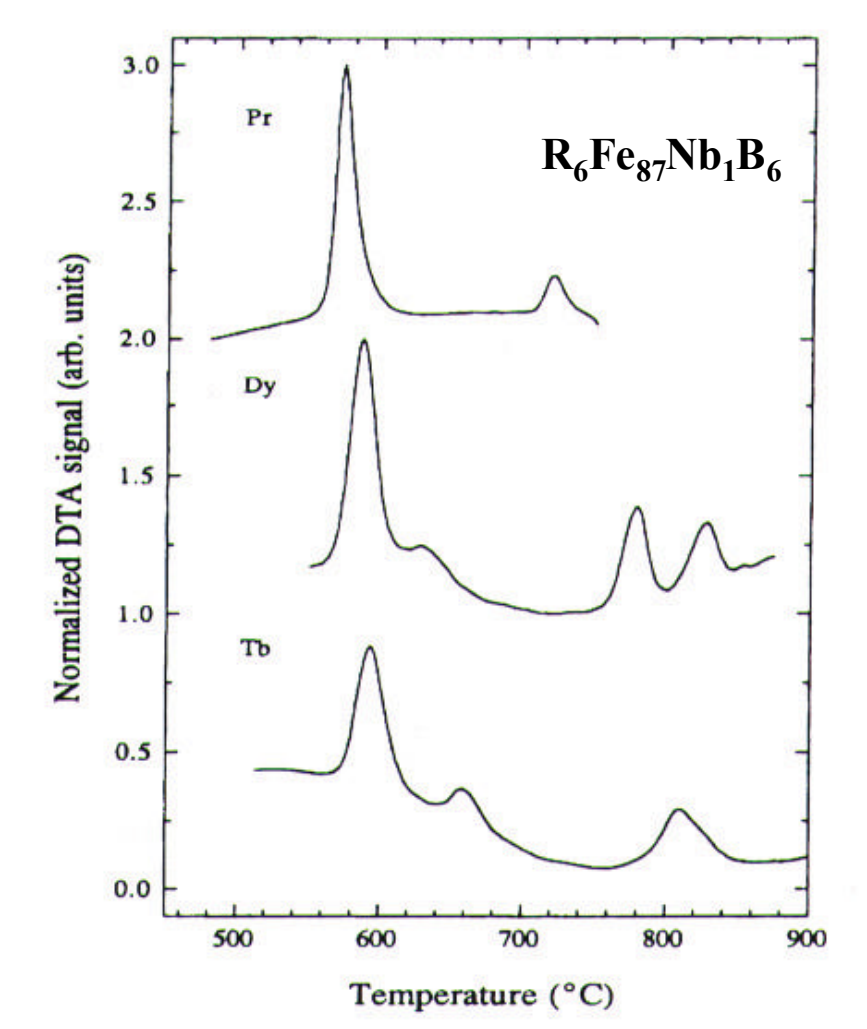

G. C. **Hadjipanayis**, J. Magn. Magn. Mater. 200 (1999) 373.

DSC – differential scanning calorimetry

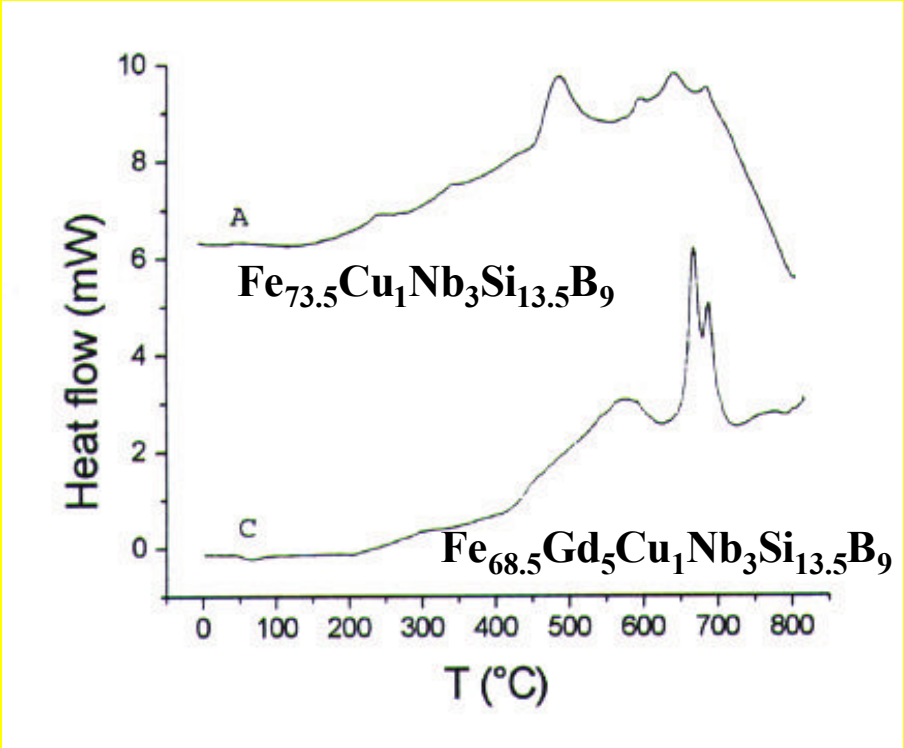

O. **Crisan** et al., ICM Rome 2003

Spin melting HARD | **Nd2Fe14B/(Fe3B, Fe) and Sm2Fe17N3/Fe** | **by** | **melt spinning or mechanical alloying**

high magnetisation of soft phases - Fe, Fe3B… + **high magnetic anisotropy of R compounds - Nd2Fe14B, $Sm_2Fe_{17}N_3$…**

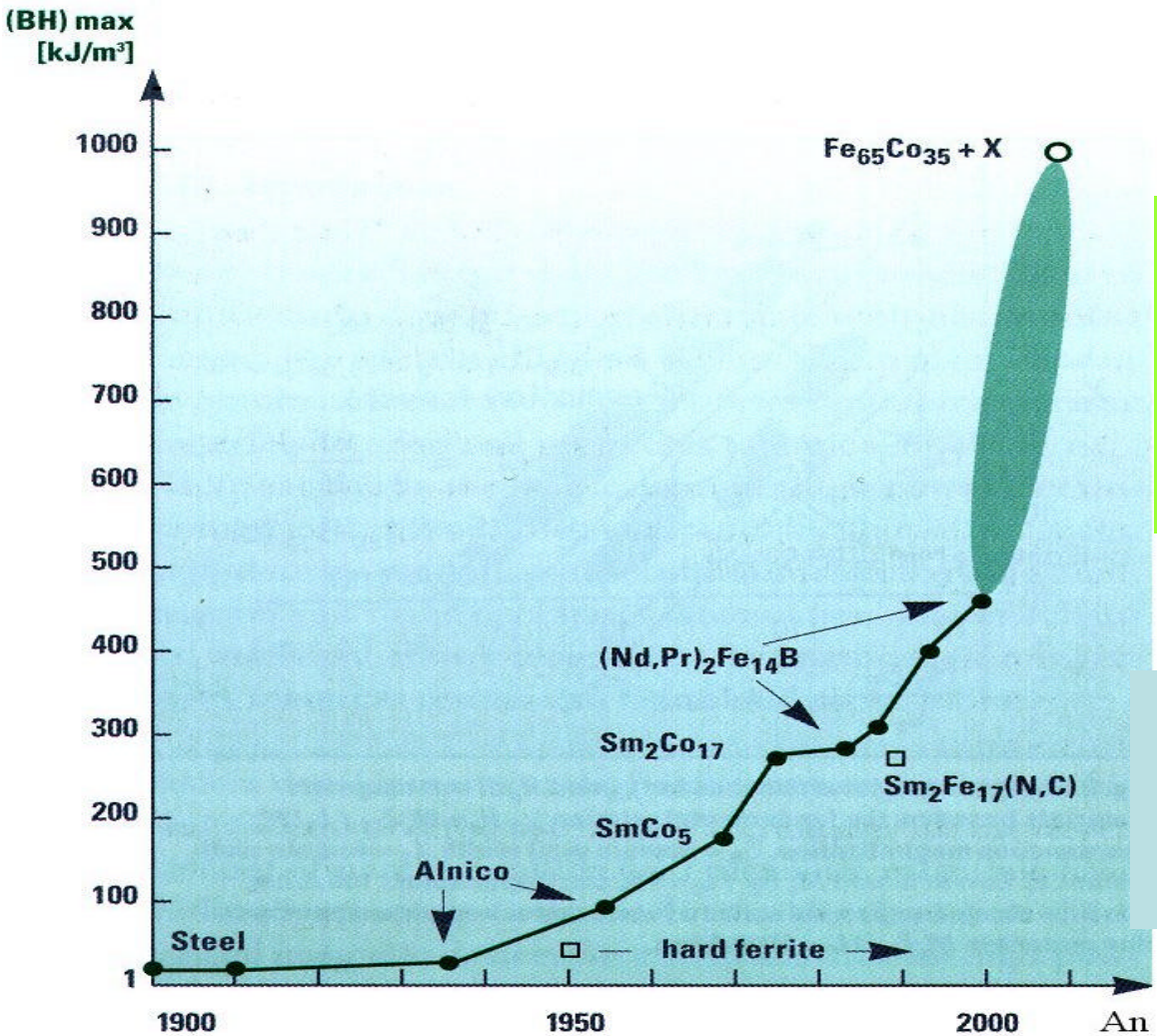

$(BH)_{max}$ = 1090 kJ/m³ for $Sm_2Fe_{17}N_3/Fe_{65}Co_{35}$ nanostructured multilayers

R. Skomski, J. Appl. Phys. 76 (1994) 7059

Kronmuller & Coey Magnetic Materials, in European White book on Fundamentel Research in Materials Science Max Planck Inst. Metallforschung, Stuttgart, 2001, 92-96

Spin melting HARD

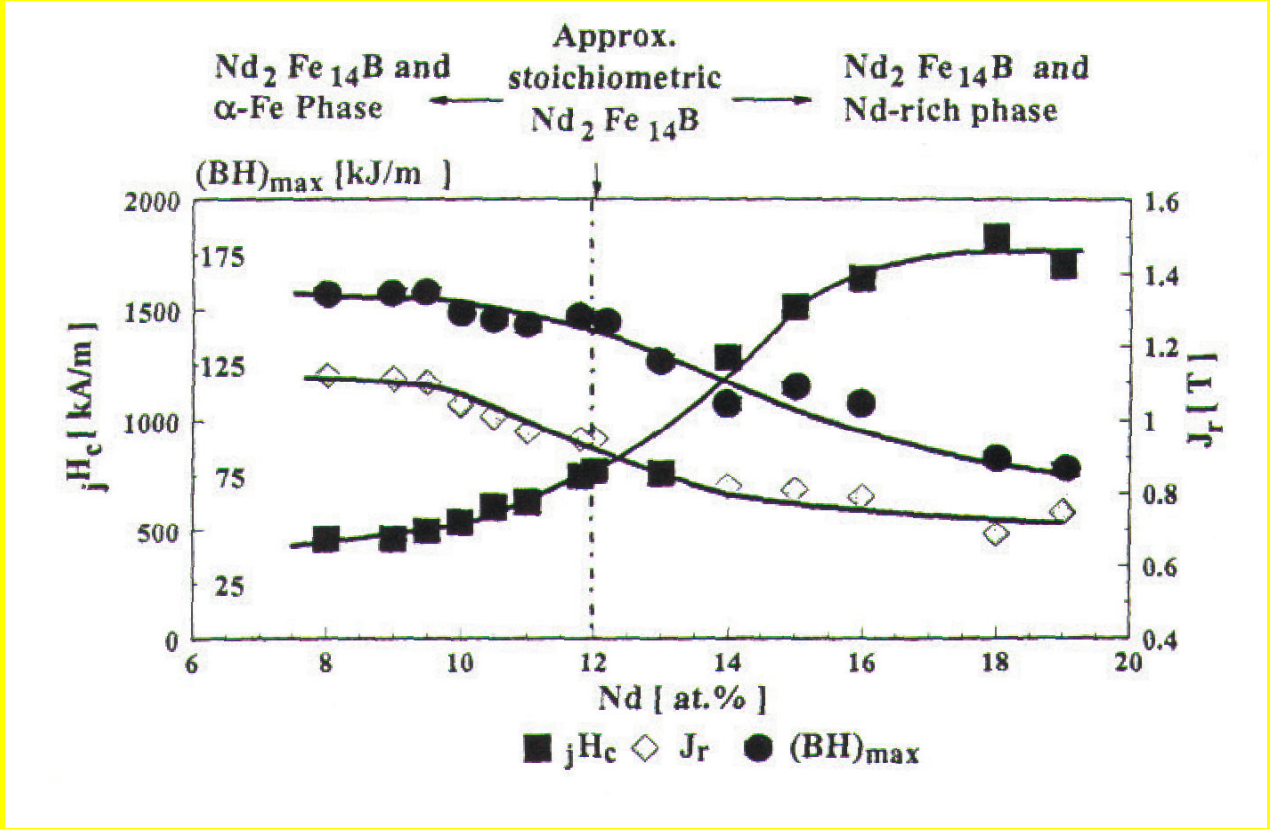

Behaviour connected to the microstructure changes in the melt spun evidenced by, TEM

H. A. **Davies**, J. Magn. Magn. Mater. 157-158 (1996) 11

Spin melting HARD

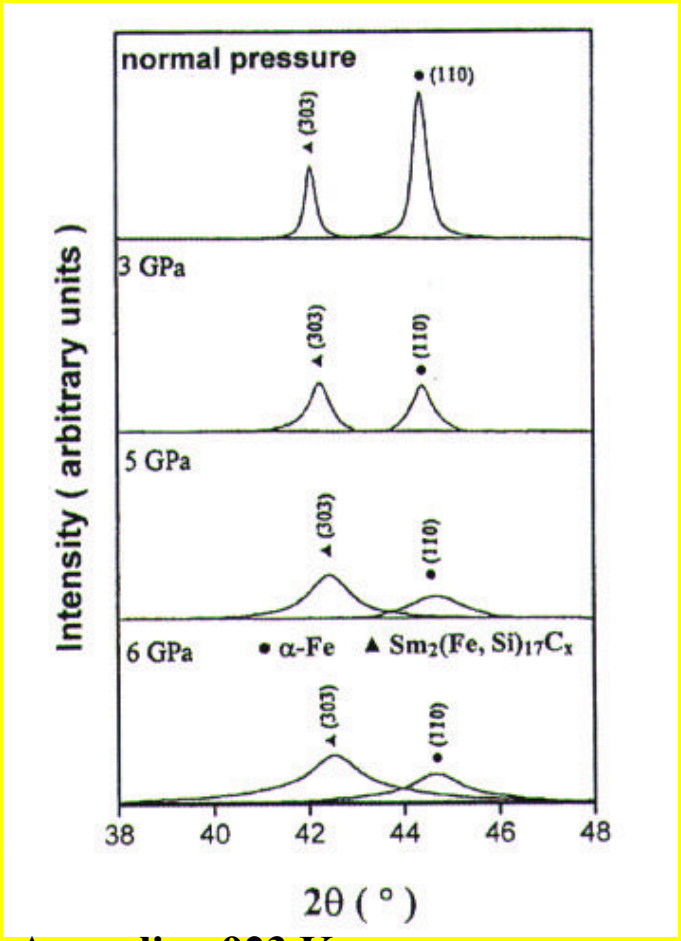

Annealing 923 K

p normal 6 GPa

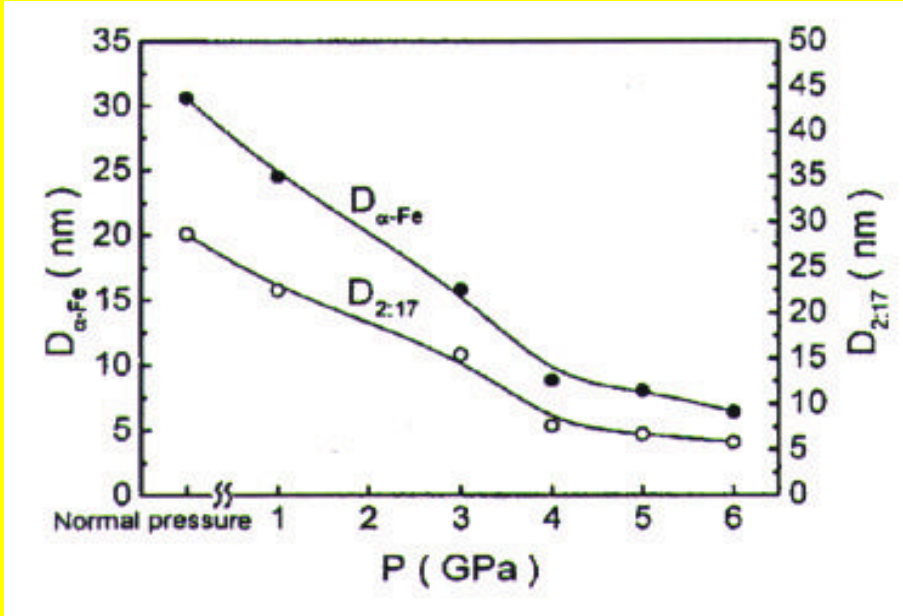

X. Y. **Zhang**, J. W. Zhang, W. K. Wang, J. Appl. Phys. 89 (2001) 477

Spin melting HARD

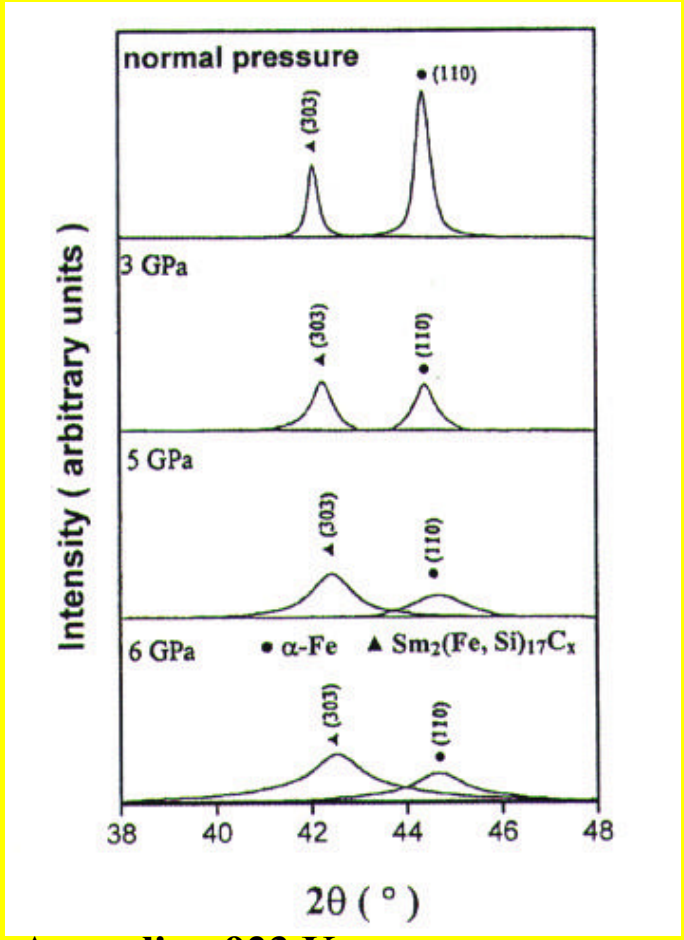

Annealing 923 K

p normal 6 GPa

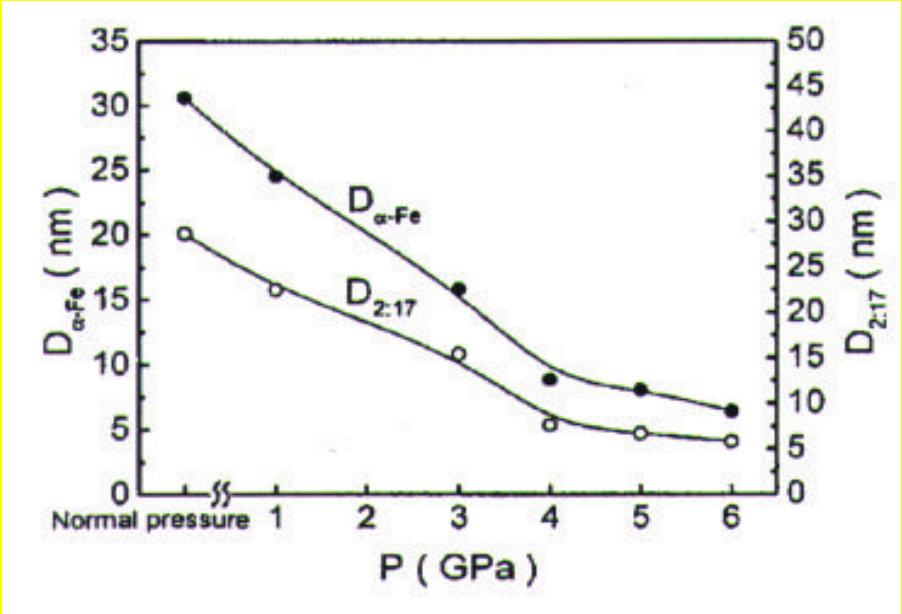

The volume fraction of $Sm_2(Fe,Si)_{17}Cx$ phase also increases as the pressure increases. This behaviour is explained by the change of the crystallisation sequence: at low pressure a-Fe is the first crystallisation phase, while at high pressure $Sm_2(Fe,Si)_{17}Cx$ is.

X. Y. **Zhang**, J. W. Zhang, W. K. Wang, J. Appl. Phys. 89 (2001) 477

Spin melting HARD

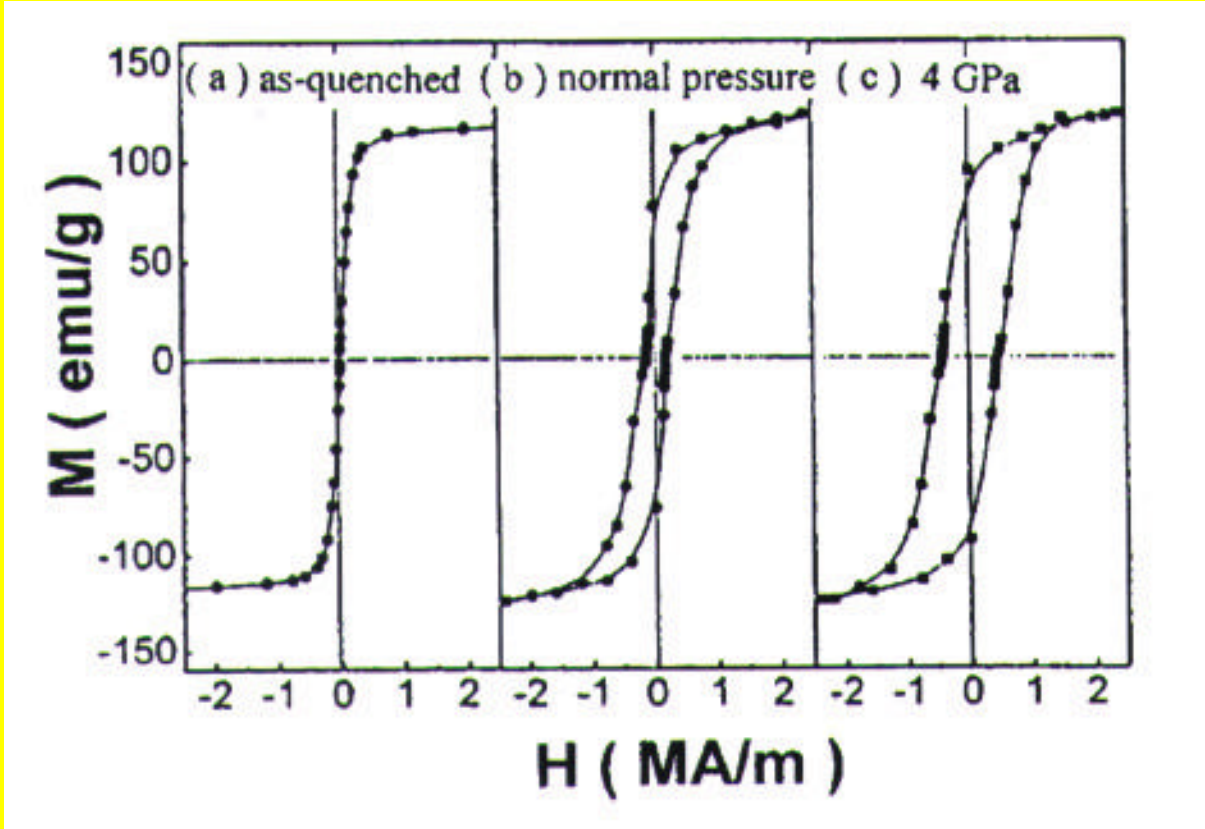

X. Y. **Zhang**, J. W. Zhang, W. K. Wang, J. Appl. Phys. 89 (2001) 477

Mechanical alloying

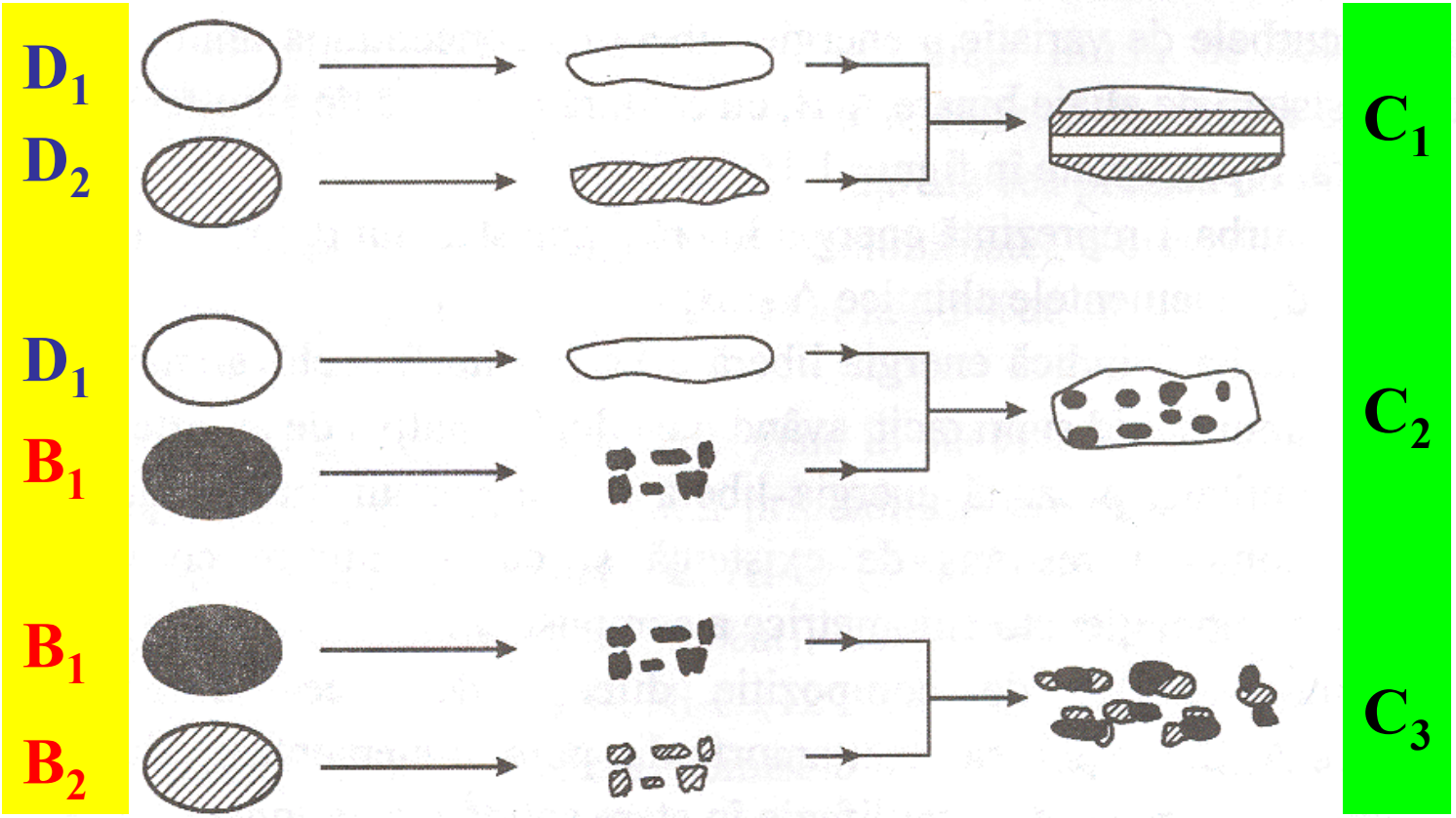

D - ductile component
B - brittle component

C - composite (compound)

MA

Mechanical alloying involves the synthesis of materials by high-energy milling

MM

Mechanical milling refers to the process of milling pure metals or compounds which are in thermodynamical equilibrium before milling

Mechanical alloying Ni_3Fe

- milling of Ni and Fe powders in a high energy planetary mill
- heat treatments (temperatures and duration)
- X-rays diffraction (XRD)
- electron microscopy
  - morphology
  - phase composition checked by EDX
- magnetic measurements: 4 - 600 K; $\mu_0 H$ £ 8 T
- Mössbauer spectrometry

The presence of the first order internal stresses acts at a macroscopic level and modifies the lattice parameters and consequently produces an angular shift of the X-ray diffraction peaks.

The second-order internal stresses act at a microscopic level of the crystallites and produce a broadening of the X-ray diffraction peaks [13, 16].

L. Castex, J.L. Lebrun, G. Maeder, J.M. Sprauel, Determination de contraintes résiduelles par diffraction des rayons X, Publications scientifiques et techniques de l'ENSAM, Paris vol.22 (1981), 51-60.
See also http://WWW.physiqueindustrie.com/

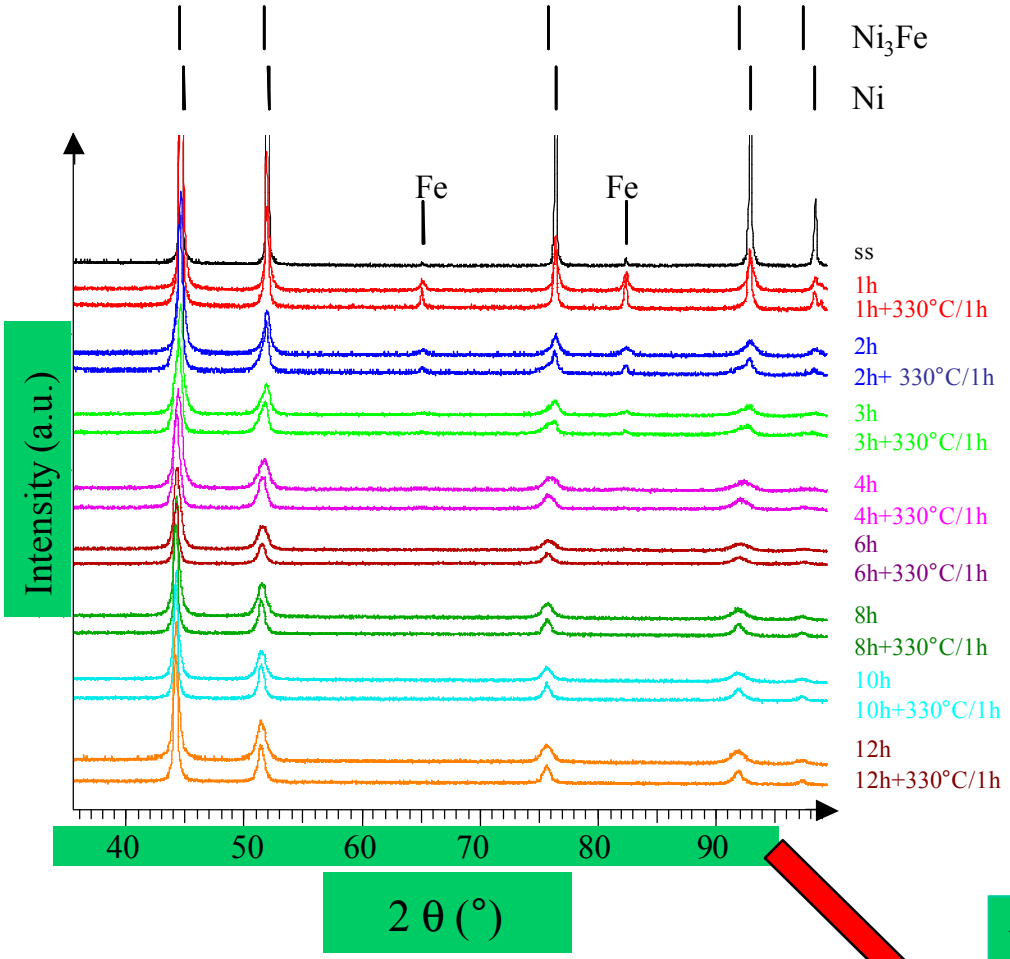

peaks shift to **lower** 2θ angles

- **Ni_3Fe** phase formation
- the **first order** internal stresses

peaks shift to **HIGHER** 2θ angles

relaxation of the first order internal stresses

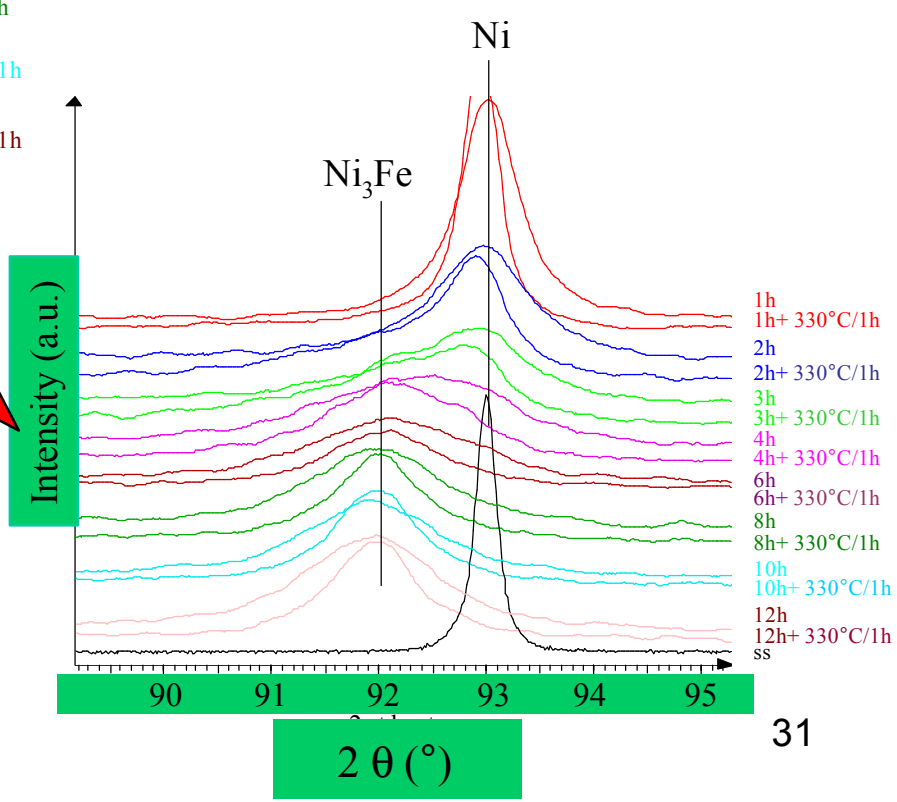

broadening of the diffraction peaks

the **second order** internal stresses

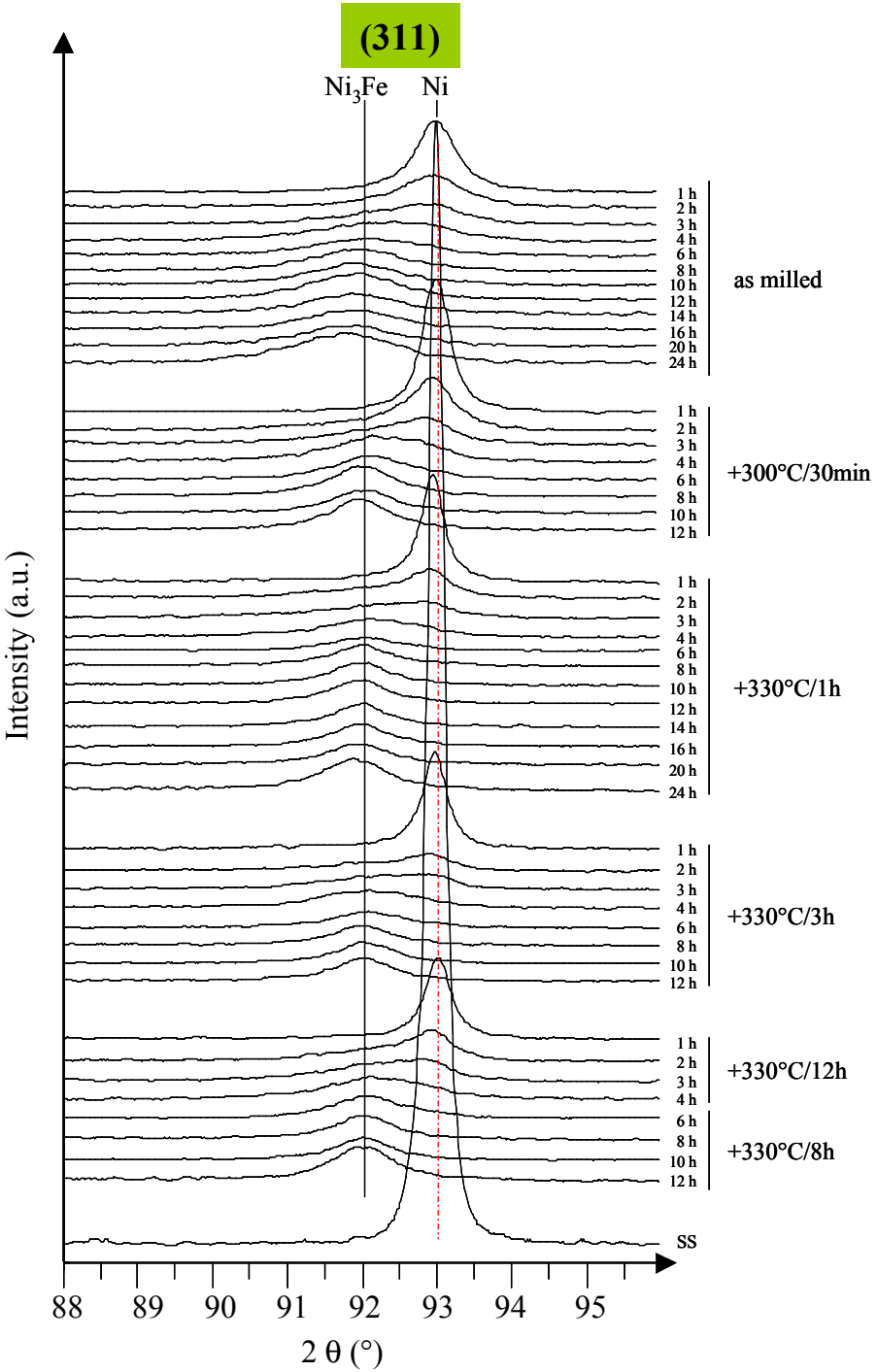

One annealing time
Different milling time

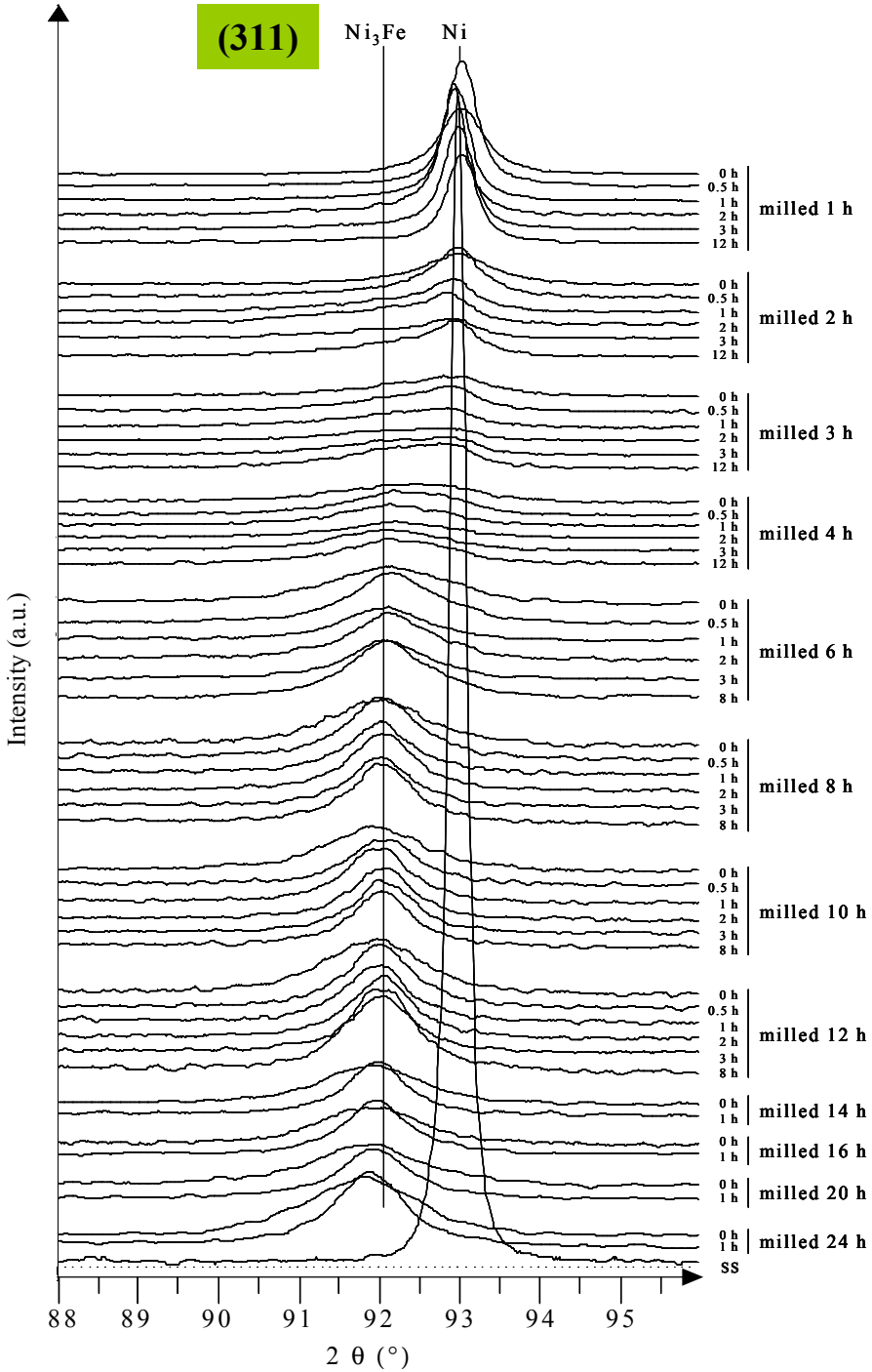

One milling time
Different annealing time

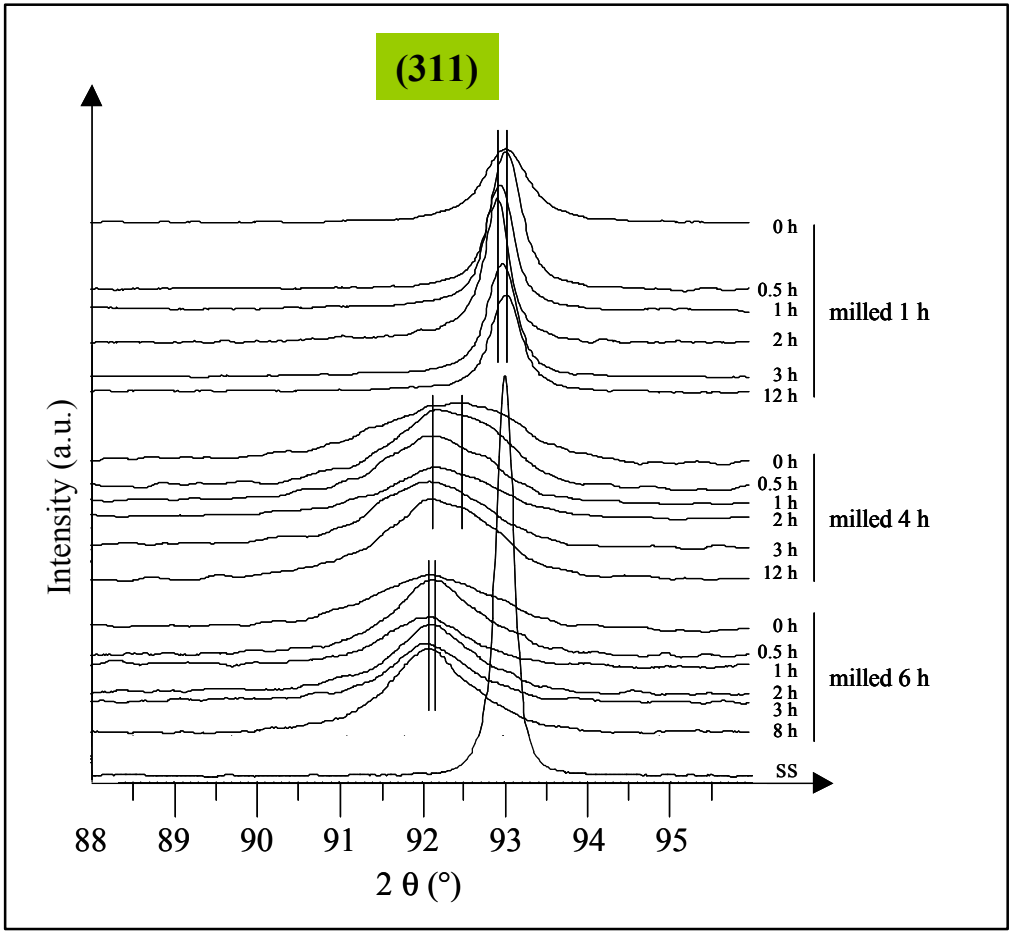

$$d = \frac{k \cdot l}{b_{\frac{1}{2}} \cdot \cos q}$$

$b_{\frac{1}{2}}$ - FWHM

$\Rightarrow$ **d** = { **12 nm** - 52 h milling; **22 nm** - 24 h milling }

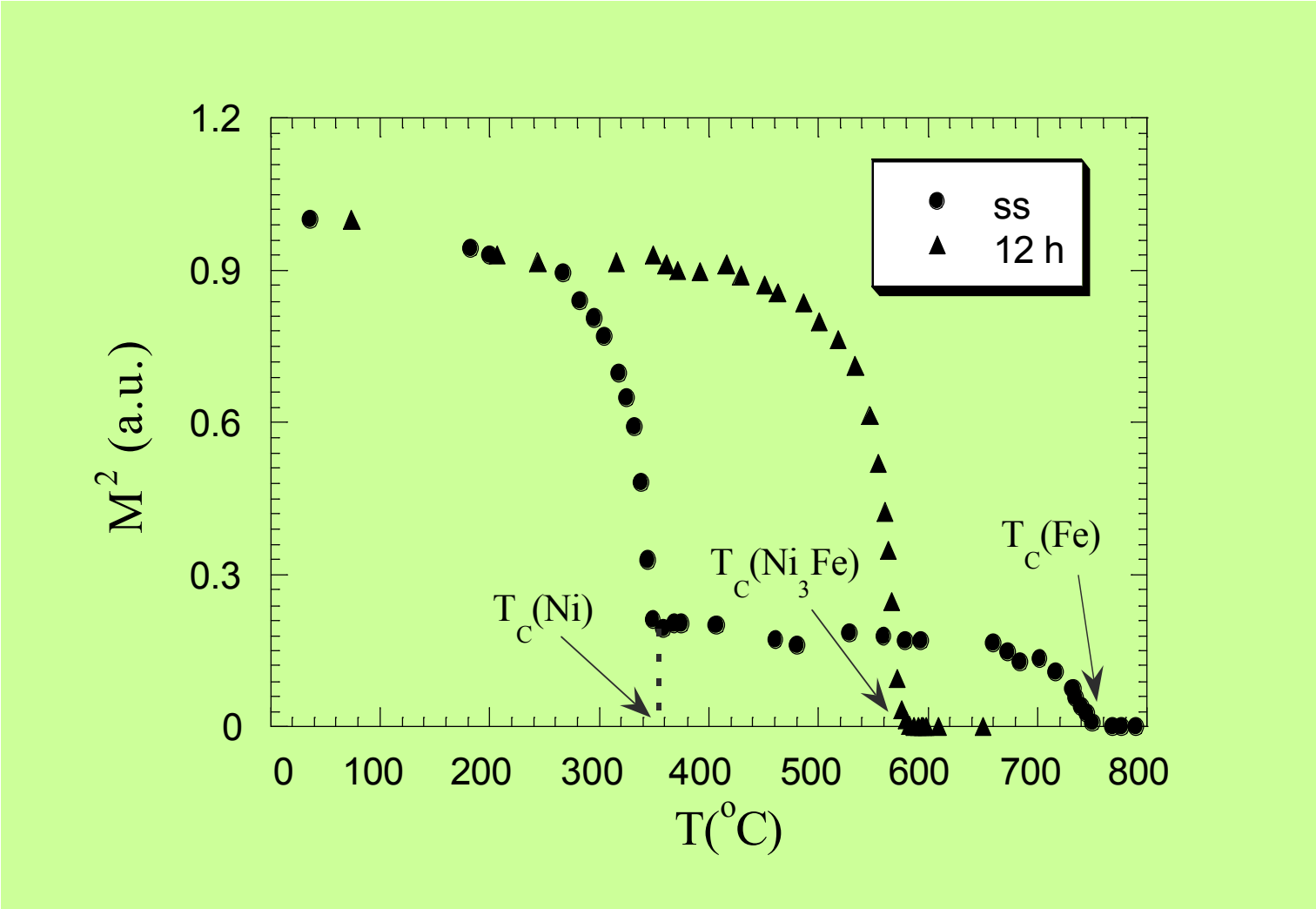
1.2
0.9
0.6
0.3
0
M2 (a.u.)
0
100
200
300
400
500
600
700
800
T(oC)
ss
12 h
TC(Ni)
TC(Ni3Fe)
TC(Fe)

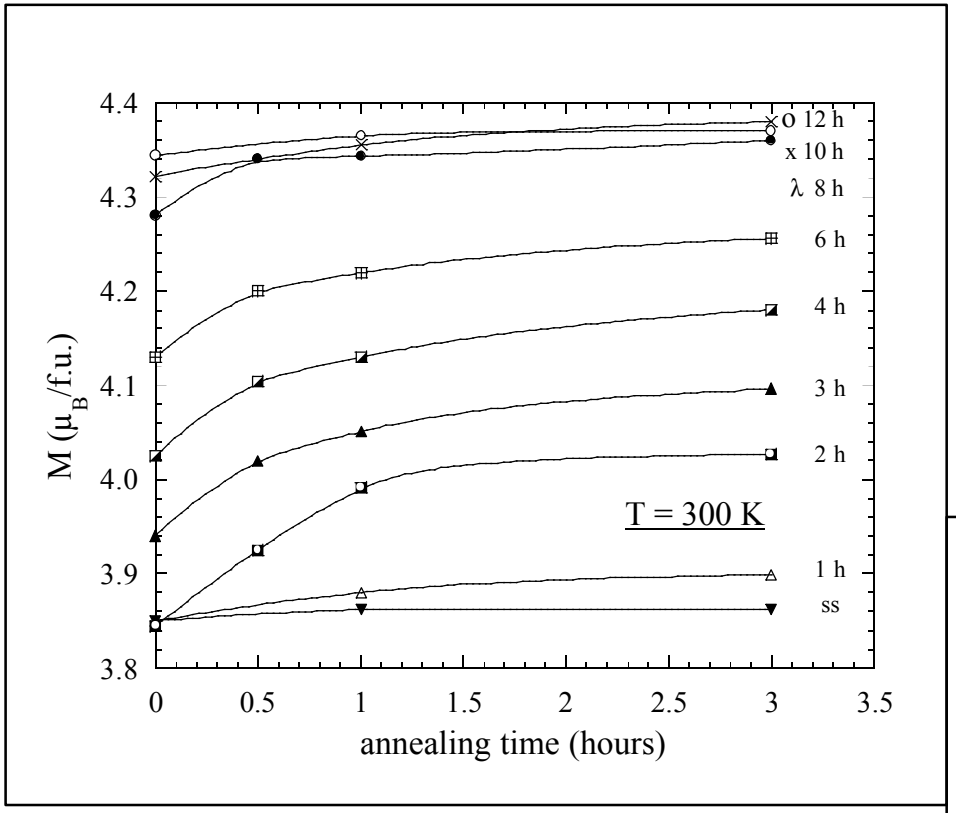

$Fe_{1-x}Ni_x$
in the reach nickel region*

x ↗ **M_{Fe}** ↗ **and** **M_{Ni}=ct.**

↓

M_{Ni-Fe} ↗ **when** **Ni_3Fe %** ↗

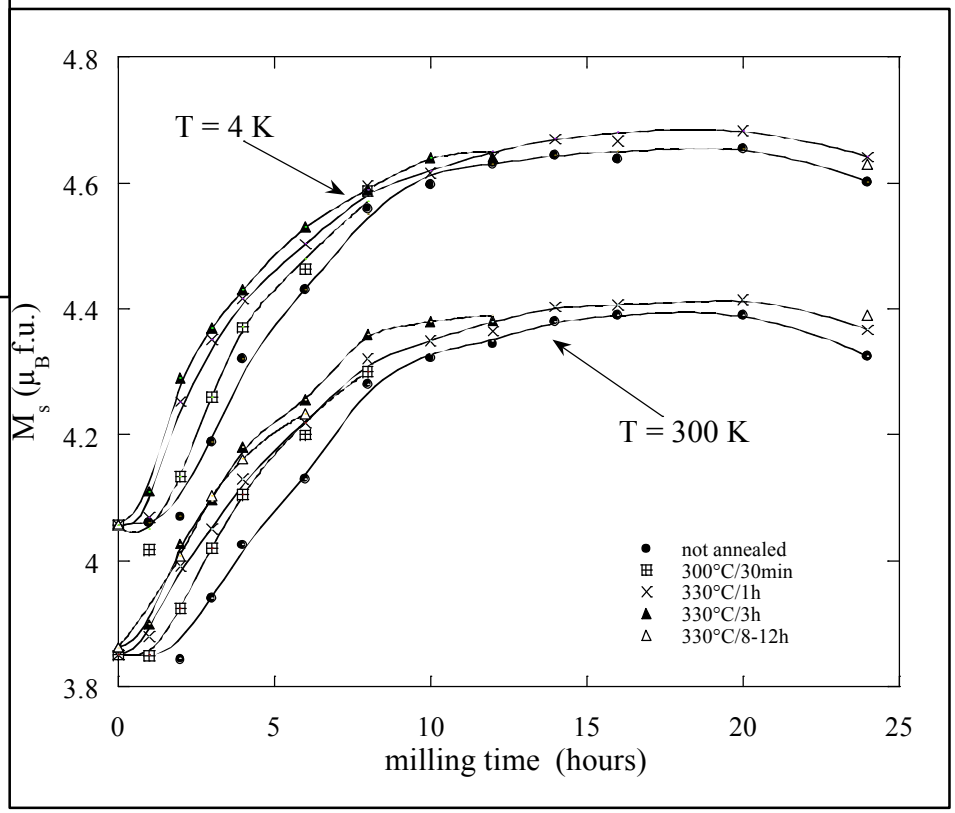

*H. Hasegawa, J. Kanamori, J. Phys. Soc. Jap. **33** (1972) 1599

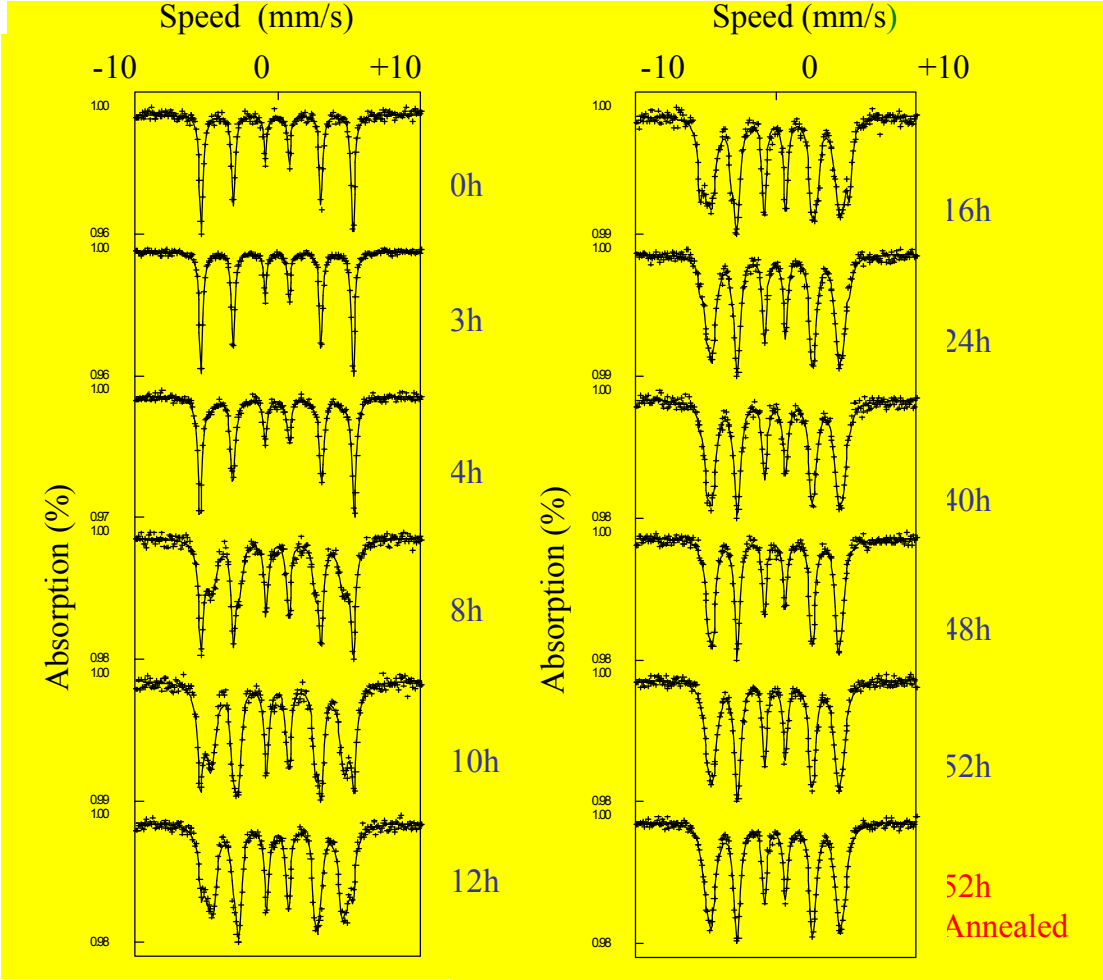
Speed (mm/s)
-10
0
+10
Absorption (%)
0h
3h
4h
8h
10h
12h
16h
24h
40h
48h
52h
52h
Annealed

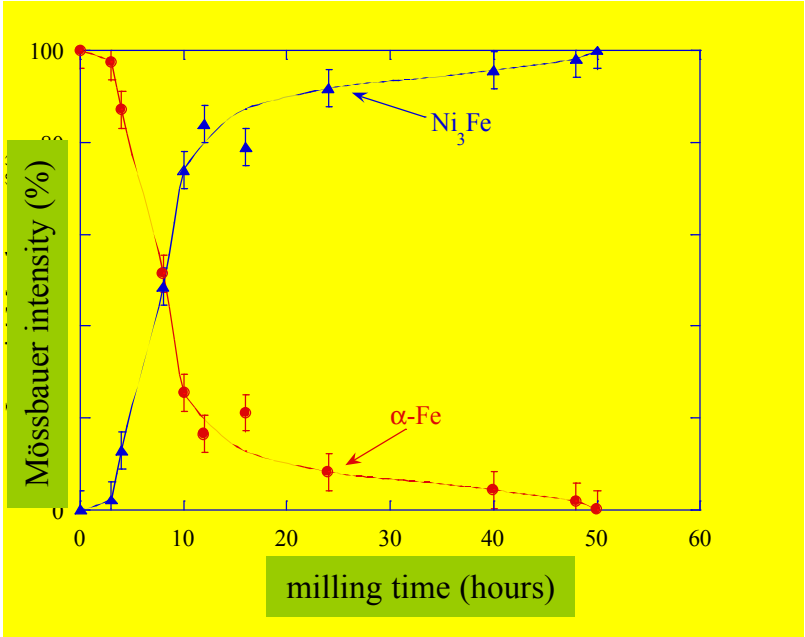
Mössbauer intensity (%)
milling time (hours)
Ni3Fe
α-Fe
0
10
20
30
40
50
60
100

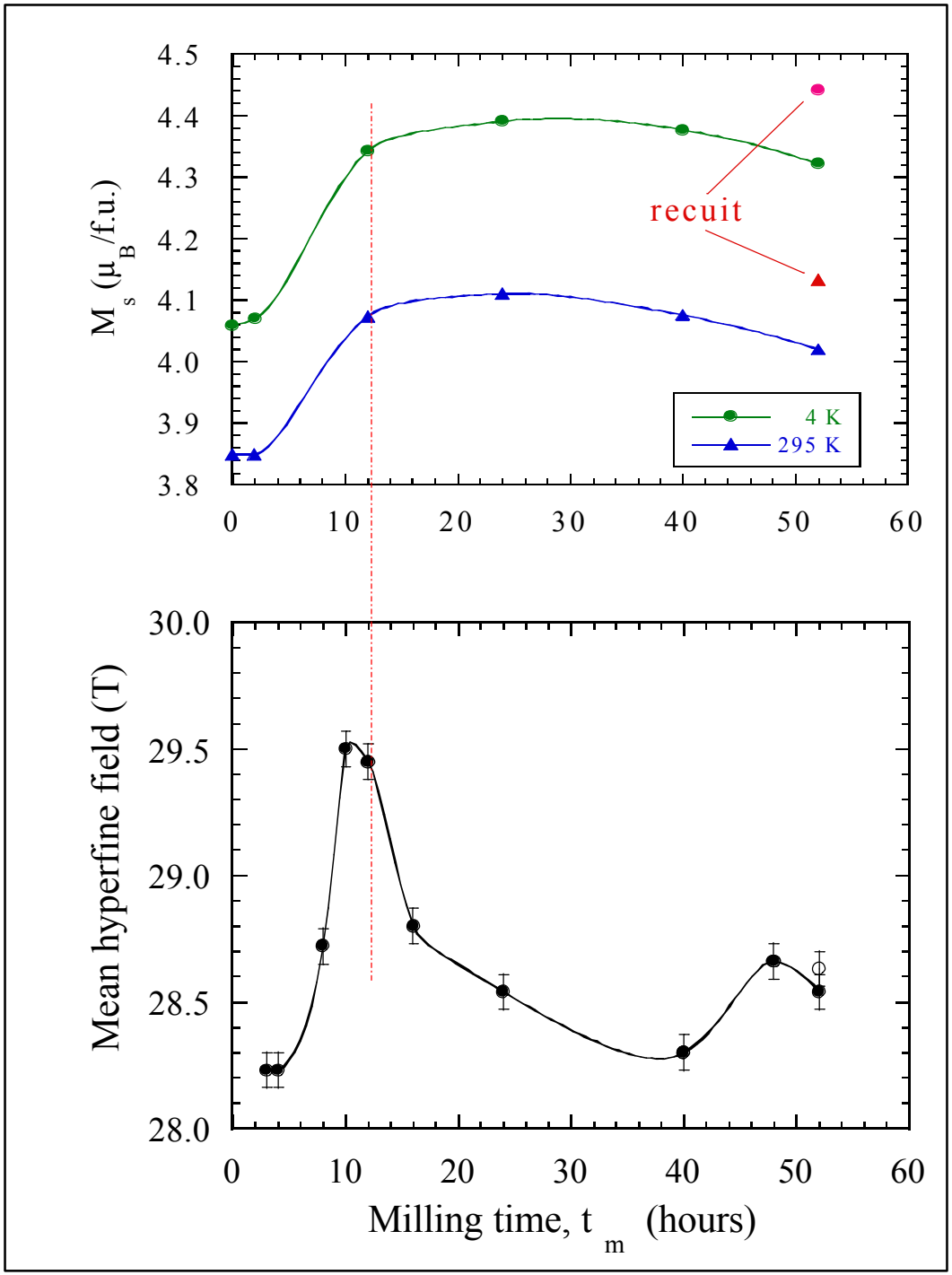
4.5
4.4
4.3
4.2
4.1
4.0
3.9
3.8
M_s (μ_B/f.u.)
recuit
4 K
295 K
0
10
20
30
40
50
60
30.0
29.5
29.0
28.5
28.0
Mean hyperfine field (T)
Milling time, t_m (hours)

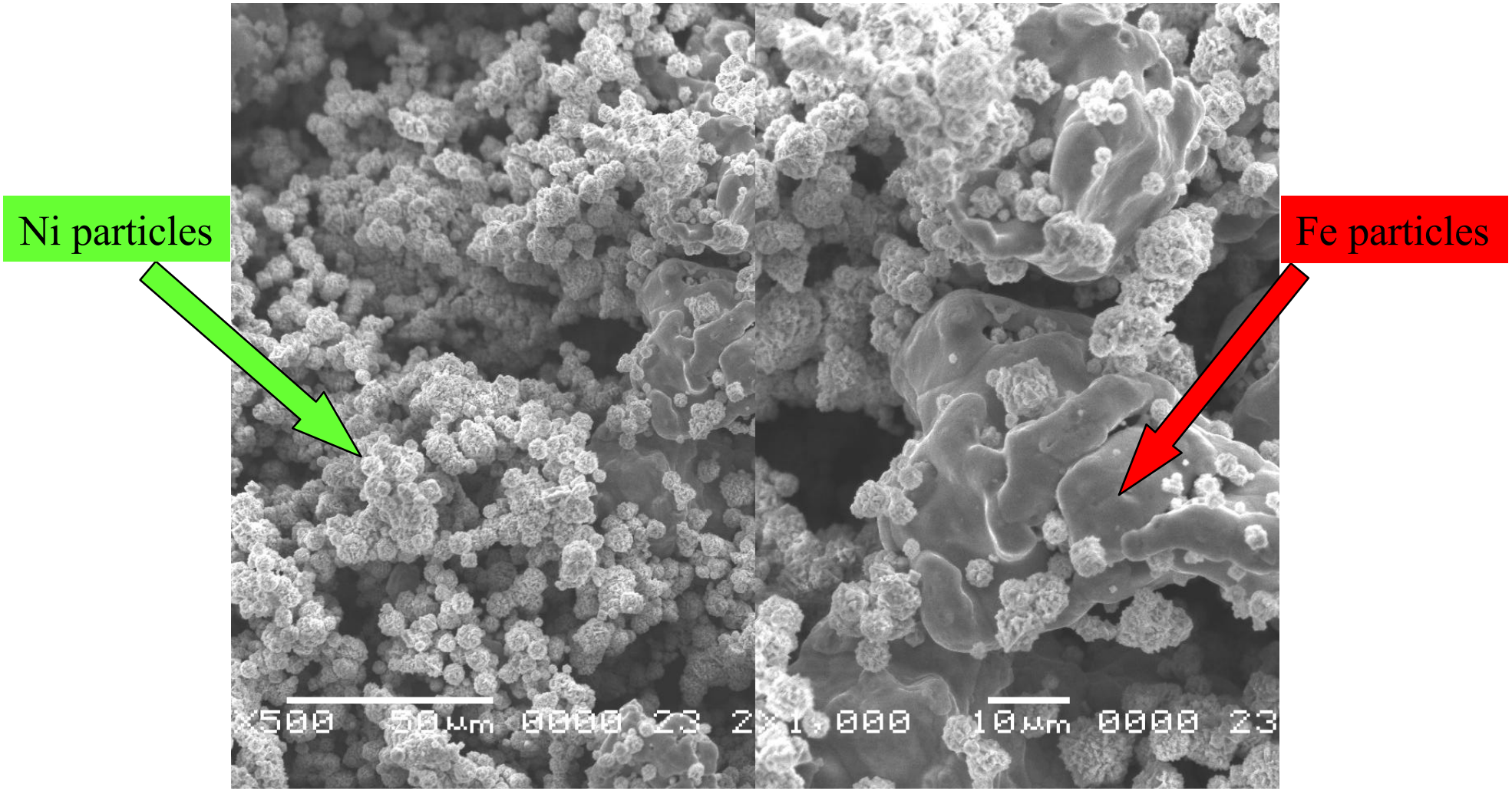

The particles morphology of the Ni75-Fe25 powders mixture
(start sample - ss)

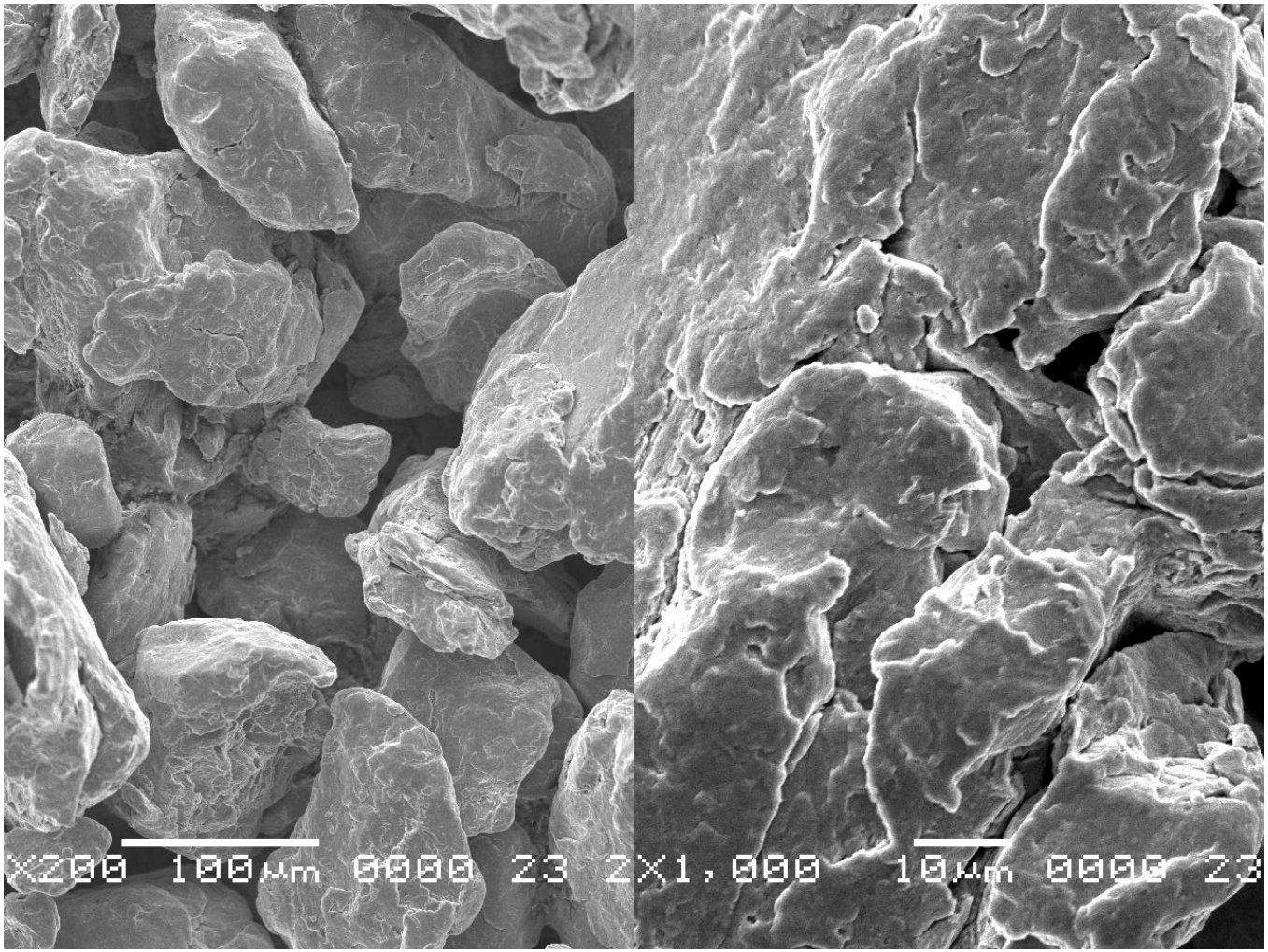

The particles morphology of the Ni-Fe powders mixture after 4h mechanical milling.

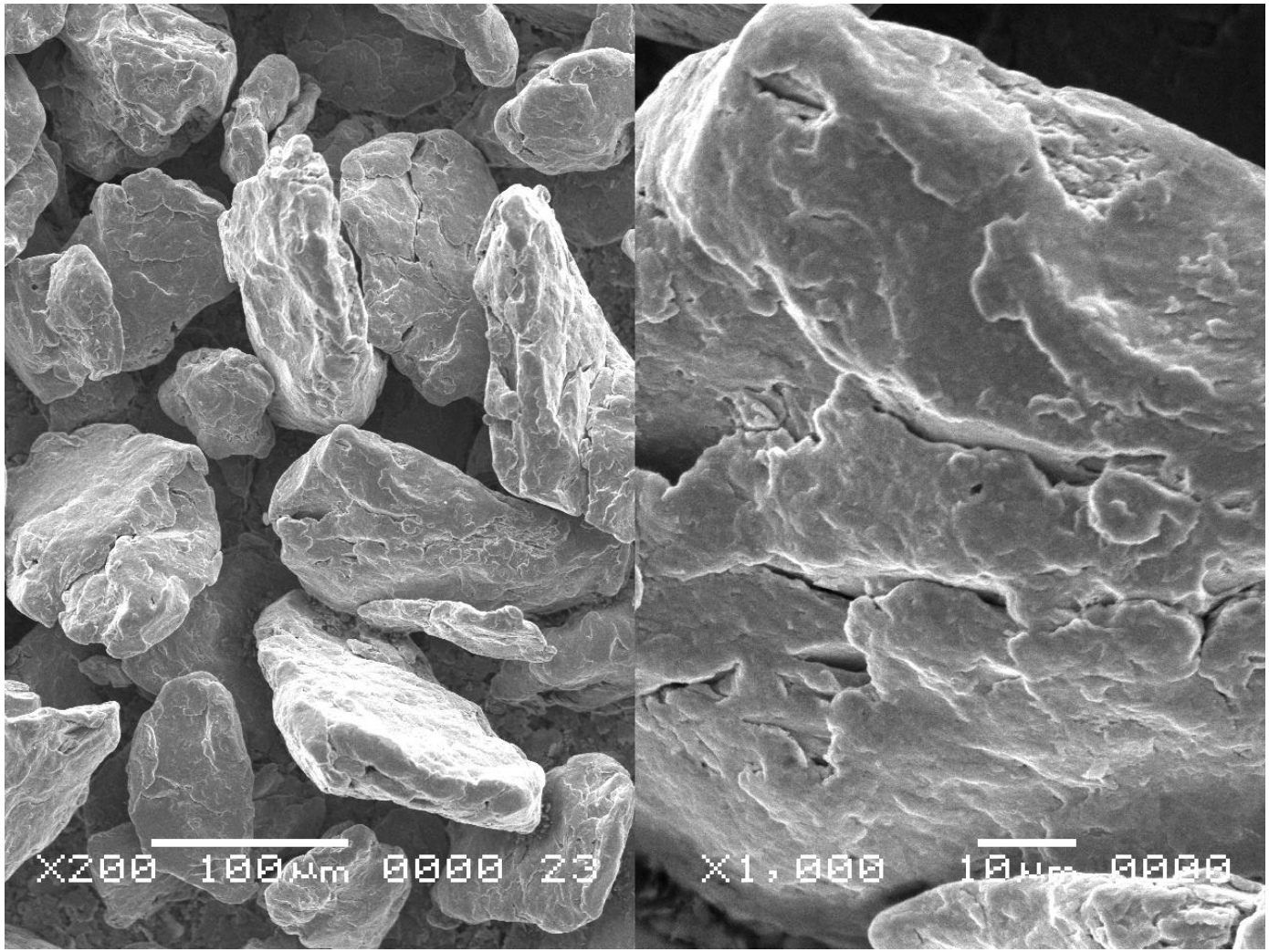

The particles morphology of the Ni_3Fe powders after 12h mechanical alloying.

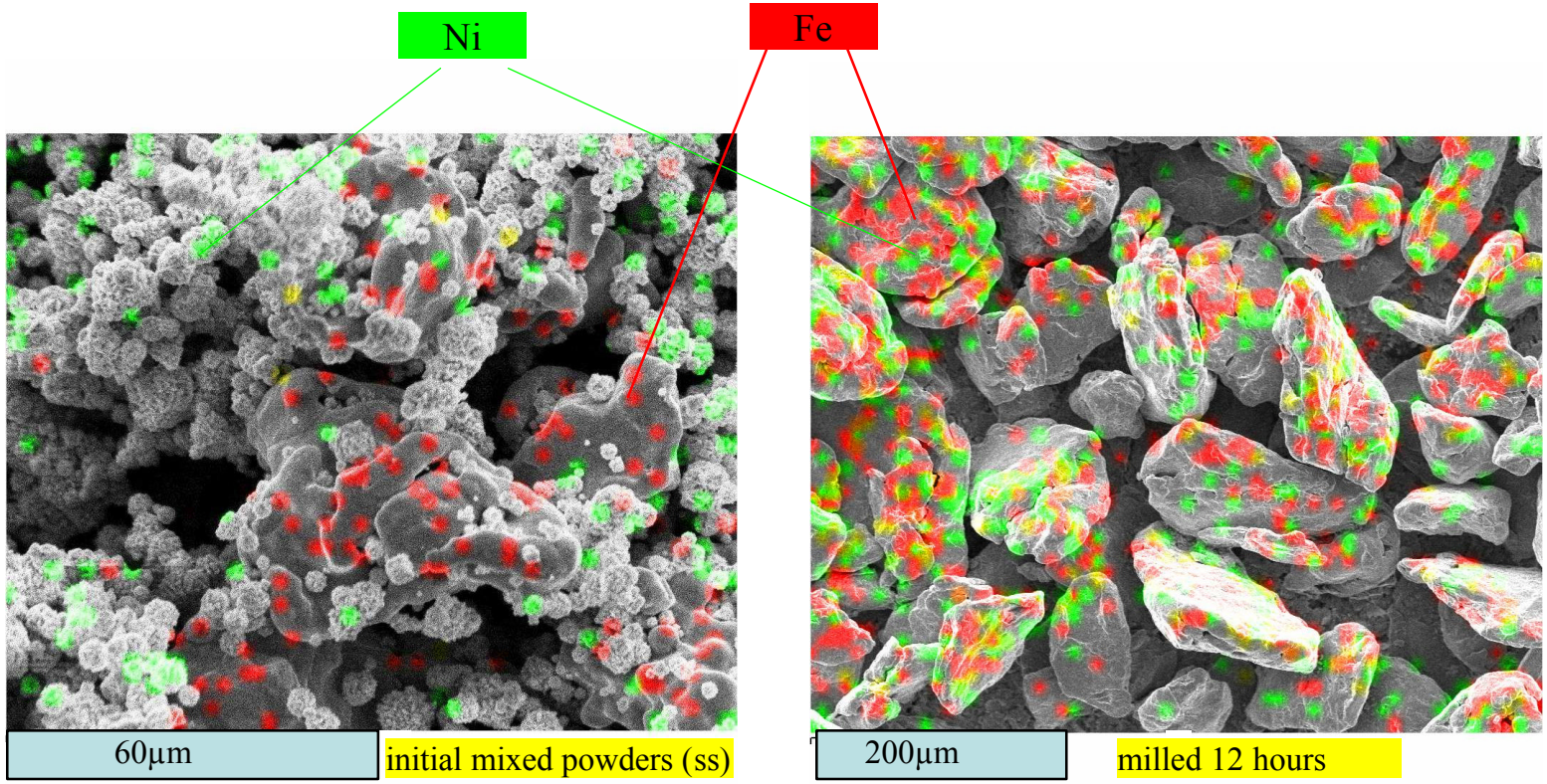

Energy dispersive X-ray analysis (EDX)

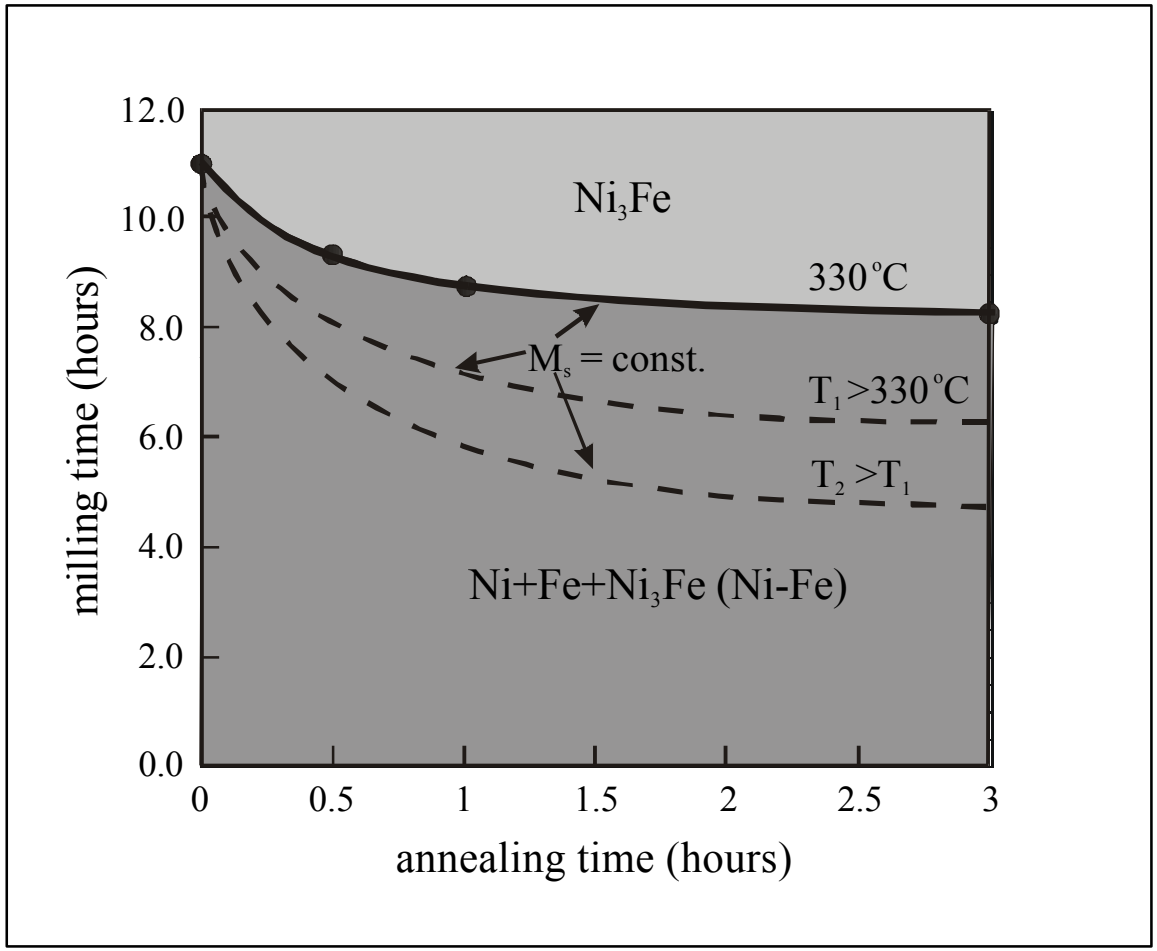

Milling – Annealing - Transformation (MAT) diagram

Table 2. Structural and room-temperature coercivity of Sm-Co-Cu-Ti intermetallic compounds

Type	Compound	Structure type	$m_0H_c(T)$
As-cast	$SmCo_7$	$TbCu_7 + Th_2Zn_{17}$	0.05
	$SmCo_{6.7}Ti_{0.3}$	$TbCu_7$	0.12
	$SmCo_{6.7}Cu_{0.3}$	$TbCu_7$	0.10
	$SmCo_{6.7}Ti0_{.3}Cu_{0.3}$	$TbCu_7$	0.15
As-cast + annealed	$SmCo_7$	$CaCu_5 + Th_2Zn_{17}$	0.12
	$SmCo_{6.7}Ti_{0.3}$	$CaCu_5 + Th_2Zn_{17}$	0.23
	$SmCo_{6.7}Cu_{0.3}$	$CaCu_5 + Th_2Zn_{17}$	0.20
	$SmCo_{6.7}Ti0_{.3}Cu_{0.3}$	$CaCu_5 + Th_2Zn_{17}$	0.26
MM + annealed	$SmCo_7$	$TbCu_7 + Th_2Zn_{17}$	0.26
	$SmCo_{6.7}Ti_{0.3}$	$TbCu_7 + Th_2Zn_{17}$	1.90
	$SmCo_{6.7}Cu_{0.3}$	$TbCu_7 + Th_2Zn_{17}$	0.70
	$SmCo_{6.7}Ti0_{.3}Cu_{0.3}$	$TbCu_7 + Th_2Zn_{17}$	2.50

M. **Venkatesan**, C. Jiang, J. M. D. Coey, J. Magn. Magn. Mater. 242-245 (2002) 1350

Chemical synthesis of FePt nanoparticles

Fe-Pt alloys are an important class of materials for permanent magnet applications because of their large magnetocrystalline anisotropy and good chemical stability.

Small FePt particles may be suitable for future ultrahigh density magnetic recording media applications.

FePt particle thin films had mainly relied on vacuum deposition techniques.

We will present here few aspects concerning chemical synthesis of Fe-Pt alloys.

Chemical synthesis of FePt nanoparticles

Sun et al. [S. Sun, C. B. Murray, D. Weller, L. Folks, A. Moser, Science 287 (2000) 1989], **in order to prepare FePt nanoparticles, have used a combination of oleic acid and oleyl amine to stabilise the monodisperse FePt colloids and prevent oxidation.**

The synthesis is based on the reduction of Pt(acac) (acac = acetylacetonate CH3COCHCOCH3) by a diol and the decomposition of Fe(CO)5 in high temperature solution.

High resolution electron microscopy (HREM) studies have shown that FePt assembly on a thermally oxidized Si substrate are well separated i.e. no agglomeration occurs. Energy dispersive X-ray (EDX) spectroscopy confirms that the average nanocrystals are slightly iron rich, $Fe_{52}Pt_{48}$, and the interparticle spaces are about 2 nm.

Chemical synthesis of FePt nanoparticles

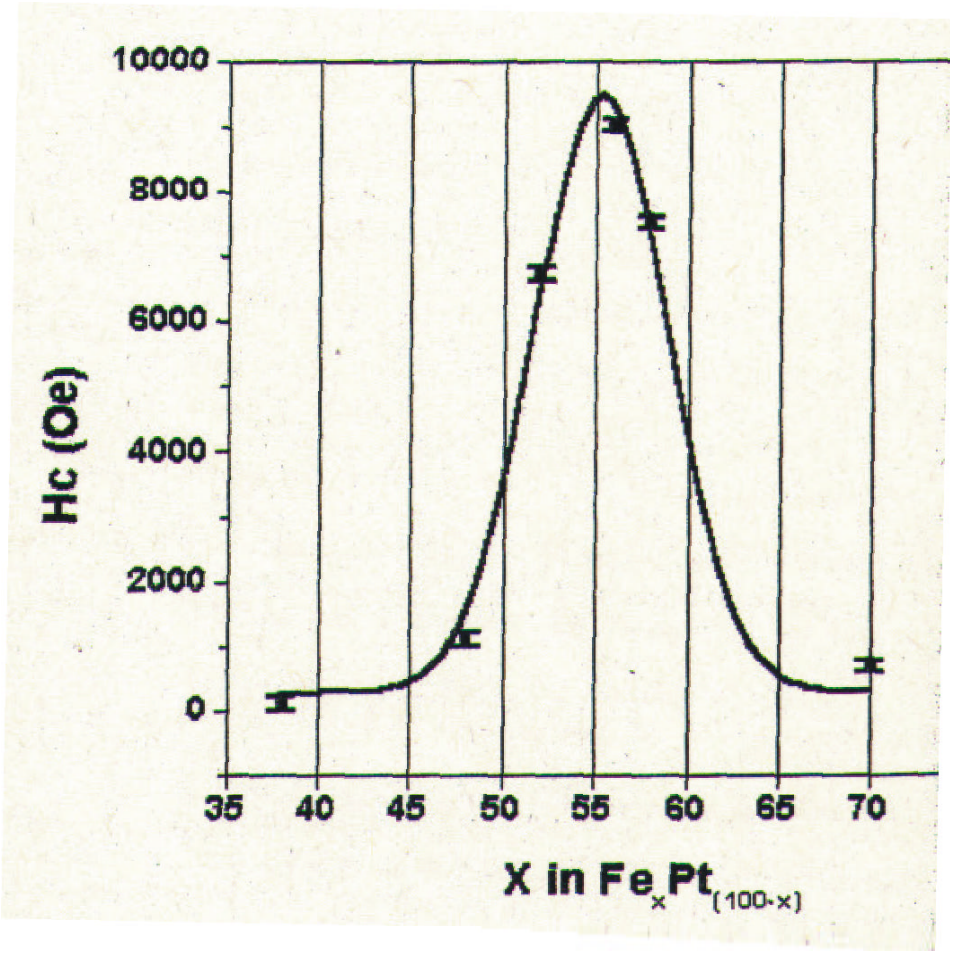

S. Sun, E. E. Fullerton, D. Weller, C. B. Murray, IEEE Trans. Magn. 37 (2001) 1239

Hexane dispersions of FePt and Fe_3O_4 nanoparticles with mass ratio in the range 5:1 to 20:1 were mixed under ultrasonic agitation.

hexane evaporation or addition of ethanol → Three-dimensional binary assembly

the size of:

- FePt = 4 nm
- Fe_3O_4 clusters = 4- 12 nm

Disordered fcc

$FePt+Fe_3O_4$ $\xrightarrow[650\ °C]{Ar+5\%H_2}$ **FePt/Fe3Pt**

Ordered fct

Soft fcc phase

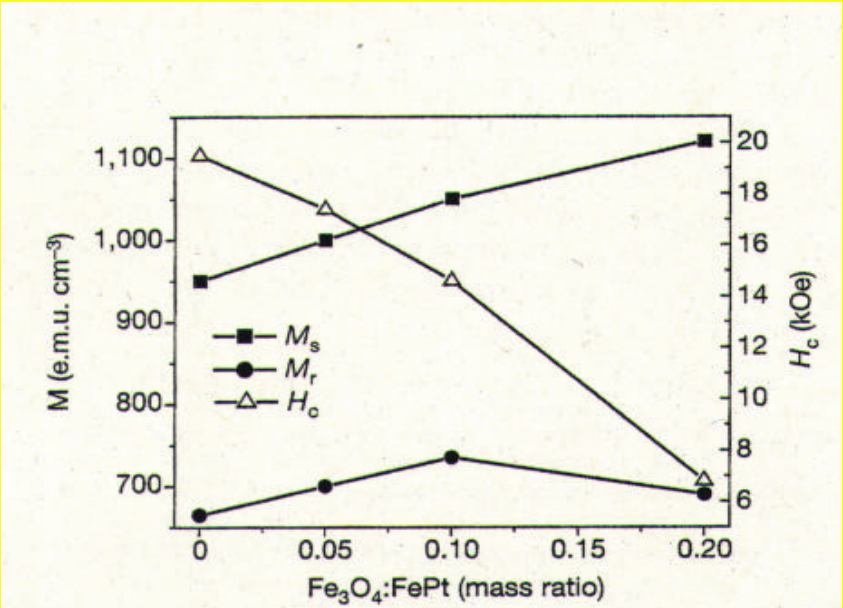

H. Zeng, J. Li, J. P. Liu, Z. L. Wang, S. Sun, Nature 420 (2002) 395

merci

thank you